

Proposed experimental study of wave-particle duality in p, p scattering

Richard M Talman

Laboratory for Elementary Particle Physics, Cornell University, Ithaca, NY, USA

(Dated: 2 February, 2023)

Of all nuclear physics experiments none are more fundamental than “elastic” p, p and, secondarily, p, d or d, d scattering. Recognizing that these particles are themselves composite, “elastic” scattering may be accompanied by temporary internal rearrangement with undetectably small energy loss. This paper argues initially that correct calculation of the spin dependence of p, p (and other charged particle) elastic scattering must account for a previously-neglected relativistic effect of “ G ”, the anomalous magnetic dipole moment (MDM) of the scattering particles. The paper then precedes to describe storage ring p, p scattering configurations capable of confirming this contention. Especially important experimentally for protons is the existence of “perfect” (greater than 99%) proton-carbon scattering polarimetric analyzing power A at $K = 183.1$ MeV laboratory kinetic energy and nearly as high nearby. Possibilities: (i) In a storage ring collider with counter-circulating proton beams, each with, say, $K = 200$ MeV energy, the final spin states of coincident scattered protons can be determined with high probability for a significantly large fraction of all scatters, both prompt and delayed. For comparison with current descriptions based on proton scattering from a hydrogen target fixed in the laboratory, this corresponds roughly, to proton kinetic energy $K = 400$ MeV in the laboratory frame, close to the pion production threshold. (ii) In a “DERBENEV-style” figure-8 storage ring, independently polarized, diametrically opposite bunches on orthogonal orbits can collide at the beam crossover point with symmetric $K'' \approx 200$ MeV energies in a slow, transversely moving frame. (iii) As another compromise, p and d beams can counter-circulate at the same time in a small racetrack shaped ring with superimposed electric and magnetic bending. In this case the scattering would be “WOLFENSTEIN-style”, with collinear incident orbits (at the cost of significantly inferior polarimetry for the deuteron beam). To investigate the consistency of quantum mechanics and special relativity it is proposed to implement options (ii) and (iii) in the COSY beam hall.

CONTENTS

I. Introduction	1	2. Luminosity estimation	16
II. Goals of the paper	2	3. Data rate estimation	16
1. Rationale	2	4. Forbidden “null detection” of T-violation	17
2. Glossary of ring acronyms and properties	3	5. Detection chamber polarimeter properties	18
III. The role of spin in low energy nuclear physics	4	VII. Unbalanced spin-flip T-violation detection	19
1. Spin tune in magnetic/electric storage rings	4	1. The lore concerning elastic p, p scattering	19
2. T-violation and identical particle treatment	5	2. Coarse integrated polarimetry averaging	19
3. Modern spin control; ancient nuclear physics	8	3. Figure-eight luminosity penalty estimate	20
4. Conjectured “prompt” p, p scattering	9	4. Anticipated data rates	20
5. Investigation of the strong nuclear force	10	5. Two particle T-violation detection	21
6. Importance of anomalous nuclear MDM G -values	12	VIII. Application of “spin transparency”	22
IV. Orthogonal collisions of paired bunches in a single beam figure-eight storage ring	12	1. History	22
1. Wolfenstein/Derbenev amplitude comparison	12	2. Adiabatic Fourier sensitivity enhancement	22
V. Paired bunch collisions in electric/magnetic storage rings	15	IX. Recapitulation and acknowledgments	23
1. Superimposed magnetic/electric bending	15	A. Consistent treatment of g, G and $g \rightarrow G$	25
2. Near perfect analyzing power	15	1. Orders of magnitude	25
VI. Low energy p, p elastic scattering search for time-reversal violation	16	2. Integer arithmetic, $g \rightarrow G$	25
1. Detection apparatus	16	B. Protons stopping in graphite	27
		References	27

I. INTRODUCTION

This paper is a companion to two published papers with related subject matter [1][2], and a planned paper on stor-

age ring studies of nuclear transmutation.

As everybody knows, for laboratory kinetic energies up to approximately 100 MeV (at which point the proton de-Broglie wavelength is somewhat greater than the proton diameter) the quantum (QM) and classical (CM) (i.e. Rutherford) descriptions of elastic p, p scattering agree splendidly. See Figure 8. This agreement clearly could not and cannot continue beyond, say, 400 MeV, when pions, unknown to Rutherford, began or begin to appear. See Fig. 6.

This failure with increasing energy has to be ascribed to one of three sources: previous ignorance of spin, of new particles such as pions, or of wave mechanics (WM) (i.e. wave/particle duality). Since the failure is sudden, while the wavelength variation is smooth, one has to blame the discontinuous behavior either on spin or on new particle threshold, neither of which Rutherford had anticipated.

For present purposes this justifies modest extrapolation of classical Rutherford treatment to higher energy, while continuing to treat “particles” as particles, rather than as waves, at least for purposes of approximate description. As regards initial beam preparation, this continues to be standard practice at all higher proton energies, even though it is misleading in some contexts, especially for charged particles such as the electron and, arguably, the muon.

One conjectures then, that semi-classical, Rutherford style Newtonian classical mechanics (CM) description can be trusted to some modest extent, for phenomenological extrapolation toward higher energy, by the ad hoc empirical inclusion of new particle thresholds as they become necessary.

An intuitively attractive way of merging these conflicting theoretical pictures is to segregate scattering events temporally into “prompt” and “delayed” categories, with the expectation that the prompt events are well described by both CM and QM, while “delayed” events require QM. Rephrasing this, one imagines “prompt events”, for which classical physics provides definitive (but eventually incorrect) results, and “delayed events” for which quantum mechanics QM is required. QM (i.e. wave mechanics (WM) at quantum, nuclear or atomic length scale) has the more challenging task of providing probabilistic “long term” description of nuclear scattering, elastic plus inelastic. Resonance, Heisenberg time uncertainty, and barrier penetration go hand in hand during the delayed phase.

In present context, it has already been shown experimentally that QM subsumes (beyond a reasonable doubt) the correct classical description of low energy Rutherford scattering. What remains to be investigated experimentally is the degree to which the segregation into “prompt” and “delayed” categories is useful.

One anticipates few surprises. Nuclear physics theory already anticipates such distinct time scales. One can scarcely improve upon the abstract of reference [7] “Two relevant time scales are introduced to describe the interplay of nuclear structure and nuclear reactions for exotic

nuclei. The collision time represents the time dependence of the external field created by the target on the projectile. The excitation time represents the characteristic time dependence of the projectile degrees of freedom due to its internal Hamiltonian. The comparison of these two time scales indicate when approximate treatments of the reaction, such as the sudden approximation, implicit in the eikonal treatment, is applicable.”¹

For prompt behavior, one expects agreement with high probability between deterministic classical treatment and probabilistic quantum mechanical treatment. On longer time scales, especially in the light of barrier penetration by “tunneling” and new particle production, one can only expect theory to produce a probabilistic description of the subsequent evolution.

This paper concentrates on the detection, in a colliding beam storage ring, of coincident scattered protons coming to rest in graphite polarimeter chambers providing nearly full directional coverage. This makes it practical to test the quantum mechanical description of low energy nuclear physics with unprecedented sensitivity.

The emphasis will be more on spin dependence than on time dependence, but curious event delays as great as 10 ns may be detectable.

II. GOALS OF THE PAPER

1. Rationale

Since its inception, between the first two world wars nuclear physics has gradually and naturally split into related but largely disjoint fields: low energy-, high energy- (or elementary particle-), astro-, cosmological-, quantum information-, and so on. There has been spectacular (but uneven) success in every one of these areas.

By now a certain natural sense of self-satisfaction, but also resignation, has developed. This is manifested, for example, by the phrase “physics beyond the standard model”. This phrase implied initially that “a correct foundation has been laid”, but has come, after many years to include “but there seems to be nothing further that can be done to check this, at least at current funding levels”.

The attitude expressed in this paper is exactly opposite; it is that “a correct foundation has not been laid, and there is plenty that can be done about it at present funding levels”. The 2022 Nobel prize “for experiments with entangled photons, establishing the violation of Bell inequalities and pioneering quantum information science” provides an example of success using this approach; especially to the extent that entanglement is interpreted as a fundamental defect, rather than a natural refinement in the interpretation of quantum mechanics and field theory.

¹ An example of “eikonal treatment” is provided by Fig. 9.

This paper concentrates on testing experimentally the quantum mechanical treatment of low energy nuclear physics, with special concentration on the role of nuclear spin in elastic scattering. This includes, for example, questioning the standard treatment of identical particles and investigating the possibility that the entanglement of scattered protons be detected. Special attention is also paid, possibly for the first time, to the influence of the anomalous magnetic moment in p, p scattering; noting, as an aside, that the adjective “anomalous” means “not understood”. See Appendix A.

For more than half a century the single most mysterious aspect of elementary particle physics has concerned the mass of the muon (μ -meson), a particle discovered by Anderson and Neddermeyer at Caltech in 1936. The muon spin was measured to be $1/2$ in 1960 by Hughes and others. Expressed as rest energy, the μ -mass is 105.66 MeV (accepting that a particle with half-life of $2 \mu s$ can have an unambiguous mass).

Already mysterious when spin was introduced was the fact that a measurably point-like particle, the electron, could have non-zero angular momentum and magnetic dipole moment. For a charged particle with 200 times greater mass, yet angular momentum corresponding to that of a heavy electron, seems to imply that the muon, too, is a point particle (lepton). Implying infinite density, this calls into question our understanding of “mass”.²

The paper is, however, primarily experimental in nature; describing in detail, accelerator designs capable of detecting possible inconsistencies in the current understanding of low energy nuclear physics, with special attention to time reversal invariance and the role of anomalous magnetic moments.

2. Glossary of ring acronyms and properties

In this paper there are enough different accelerators, with unfamiliar acronyms, to justify introducing them now, in one place. COSY is a low energy proton or deuteron storage ring in Juelich, Germany, whose days are numbered. Reference [10] is a long and detailed CERN yellow report, slightly pre-dating COVID, which describes PTR as a prototype ring proposed to be built in the COSY beam hall, along with a bunch accumulator BA. By retaining existing equipment, especially injection, already functioning in COSY, a substantial fraction (perhaps $1/3$) of the value of the next generation installation in the COSY hall would be saved. Figures in this

paper show the COSY beam hall with arc elements in their current locations, but with altered straight sections.

Two (mutually compatible) storage ring designs are described, which have been produced during the COVID “hiatus”. One is shaped like a race-track, the other like a figure-8. Though these rings cannot operate at the same time; to switch from one to the other operation can be expected to be routine. Together, they are more powerful than had previously been contemplated. Furthermore, these designs retain a much larger fraction of the current COSY installation; as already mentioned, the circular arcs of the COSY ring are retained in plane, common to both storage rings, and injection can be retained as-is. Yet $2/3$ of the value invested in COSY in the past is now retained.

Figure 1 provides a skeleton view of a figure-eight storage ring for which a more detailed design is shown in Figure 2. We designate this configuration as DERBENEV who introduced figure-8 design based on spin consideration. Most significant of this configuration for present purposes is the fact that a single beam can “collide with itself” or, rather, that bunches separated by half the circumference collide at the crossing point, with orthogonal incident orbits. *This feature of DERBENEV configuration contrasts with all previous scattering configurations for which colliding bunch orbits are collinear.*

A second ring design, referred to as WOLFENSTEIN racetrack, is shown in Figure 3. Simultaneously counter-circulating beams (for example clockwise protons and counter-clockwise deuterons) are supported. This requires electric bending superimposed on the existing magnetic bending, as illustrated in Figure 4.

Yet another figure-eight design is shown, at the top of Figure 5. It is the JLEIC-BOOSTER injector accelerator as had been intended for the Jefferson Lab electron-ion collider. At the bottom of the same figure is a graph showing JLEIC-BOOSTER lattice functions. These figures apply to the BOOSTER component in the Jefferson Lab electron-ion collider, JLEIC injector line. Since this figure-eight ring has roughly the same size as the previously introduced COSY hall rings, and serves comparable beam energies, the ring elements and lattice optics can be expected to be similar to the lattice functions shown.

Also shown, in Figure 4, is an illustration of an insertion constructed by Grigoriev and others, whose purpose is to superimpose electric bending within every existing COSY bending magnet. It is this electric/magnetic superposition which will enable the simultaneous co- and counter-circulation of stored beams. This capability is required to implement item (iii) of the abstract.

² Reading just the thirteen pages of Chapter 2 of the Max Jammer book “Concepts of Mass”, one may be surprised to learn that, as recently as the time of Archimedes, the Greeks had a correct understanding of *specific gravity* while, at the same time, no concept of *density*. With no concept of mass, there can be no way to conceive of density. For us, except for being expressed in different dimensional units, we consider specific gravity and density to be essentially identical material properties.

PTR OPERATION as POLARIZED p,p COLLIDER

ALL COSY INJECTION, BEAM AND SPIN CONTROL IS PRESERVED
 THERE IS NO ACCUMULATING EDM SIGNAL
 BEAM HAS VANISHING SPIN TUNE
 POLARIMETER: $0.8 < A < 1.0$, for $E \sim 0.01$

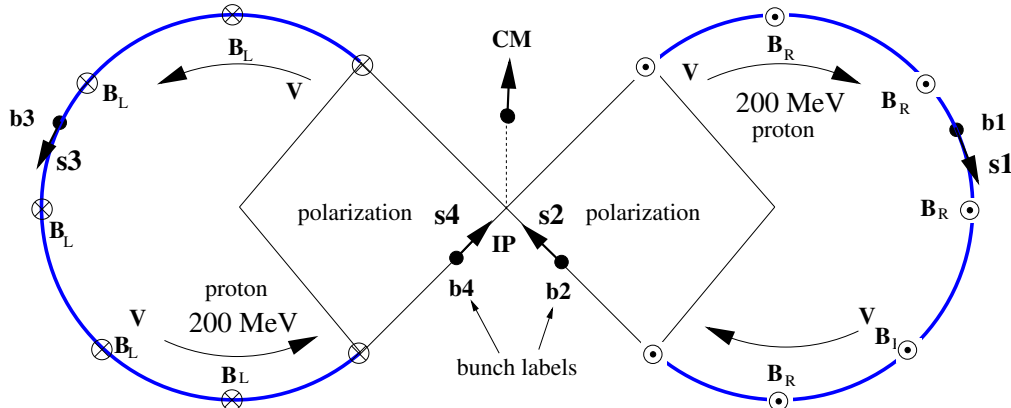


FIG. 1. Skeleton design plan for a 200 MeV (kinetic, laboratory) energy polarized p,p figure-eight collider. Since the global spin tune vanishes ($Q_s = 0$) bunch polarizations can be set independently and can be phase locked (shown pointing forward as s_2 and s_4 for bunches b_2 and b_4) to remain frozen indefinitely. *Two beams cannot counter-circulate at the same time.* But beam circulation direction can be reversed with frequency domain setting and re-setting precision, without the need for (impractically precise) electric and magnetic field measurement. This is almost as useful as simultaneous counter-circulation for reducing significant systematic errors by averaging over reversals. Both incident beam spins states at the collision intersection point (IP) can be pure, and each scattered particle momentum and polarization are measured with maximum possible (100%) analyzing power as each it slows through 183 MeV energy.

III. THE ROLE OF SPIN IN LOW ENERGY NUCLEAR PHYSICS

1. Spin tune in magnetic/electric storage rings

With novel experimental treatment of spin being emphasized, it is useful to review properties of spin as they are understood in accelerator physics. All that is needed is the concept of spin tune “ Q_S ” (where the unconventional subscript “S”, to be replaced immediately by “E” or “M”, here serves only to disambiguate from “charge”) of a (topologically circular) storage ring. The “topologically circular” generalization here means (much as in Ampère’s circuital law) that the ring can be elliptic or racetrack-shaped, or any other closed, singly-connected planar (2D) shape, without changing the numerical value of spin tune Q_S .

For a so-called “Dirac” particle in a purely magnetic field, with spin directed, say, in the horizontal forward direction like a headlight, the spin remains always horizontal and forward. For any particular particle type, Q_M , (which can have either sign) is a measure (as a fraction of 2π of the spin’s horizontal angular deviation, relative to the particle direction, after one complete revolution. For a non-relativistic Dirac particle $Q_M = 0$. Irrespective of the value of Q_M , the vertical component of the spin of a

particle moving in 2D is conserved.

Eq. (3.7) in reference [2] provides formulas for spin tunes in purely electric and purely magnetic rings as

$$Q_E = G\gamma - \frac{G+1}{\gamma}, \quad Q_M = G\gamma, \quad (1)$$

where γ is the usual relativistic factor and G is the “anomalous MDM”.

Values of G for low mass nuclear isotopes are given in Appendix A. This appendix addresses several incidental issues, including the following:

1. Explanation of the relationship between “magnetic g-factor”, g , and “anomalous MDM”, G ;
2. Explaining why both g and G can be usefully approximated by rational ratios n/d of positive integers n and d , where d is not allowed to exceed some large value, 100, for example, chosen to be consistent with the precision with which the isotope mass is known and, for unstable isotopes, the number of turns in a storage ring that the isotope can be expected to survive.
3. The rational fraction representations of G provide the fraction of 2π precession caused by anomalous MDMs. Because of the motion-induced rest frame

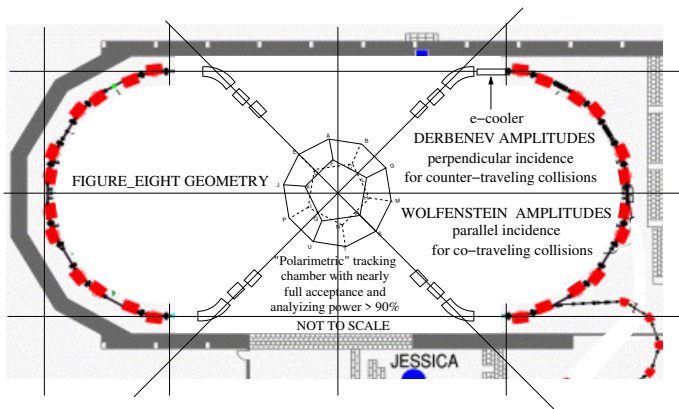


FIG. 2. This layout figure shows COSY (as of 2022) after incorporation of the superimposed electric bending shown in Figure 4. The semicircular arcs are preserved exactly as present, except the arc magnets are powered individually, to compensate appropriately for the superimposed electric bending. “Co-traveling bunches” (needed for resonant nuclear transmutation) have same sign, parallel incident momenta. “Counter-traveling bunches” (needed for p, p scattering) also have parallel incidence momenta. The detection chamber situated at the crossing point is shown on the right side of Fig. 3

magnetic field caused, for example, by elastic scattering of one proton by another, this precession causes spin evolution, proportional to scattering angle, whose presence would otherwise be interpreted as violation of time reversal invariance.

4. Since the evaluation of g and G depend on isotope mass it is important for the same exact mass to be used in their separate evaluations and, furthermore that they be represented by dimensionless ratios (such as mass number A , or a nearby value incorporating the mass defect..
5. Furthermore, for high precision determinations it is essential to use “integer arithmetic” (meaning no decimal points) in the application of the conversion formula ($G = g \times m/Z - 2$)/2), thereby preserving rational relationships.

Though one thinks intuitively, of particle MDMs as parameterizing precession in a magnetic field, in the rest frame of a charged particle moving at any non-vanishing velocity in a transverse electric field there is a non vanishing magnetic field, which causes “in plane” precession in the plane perpendicular to the magnetic field. This is the source of non-vanishing spin precession of an electrically charged particle moving in a transverse laboratory electric field.³

³ Though it is rarely (if ever) noted, the precession of a charged particle spin in a transverse electric field is, in some sense, “dual” to the Stern-Gerlach deflection of the orbit of a charged particle moving in a (non-uniform) magnetic field.

In the current (only weakly relativistic) context, as $\gamma \rightarrow 1$, these tunes can be approximated by their limiting values;

$$Q_E^{1 \leftarrow \gamma} = -1, \quad Q_M^{1 \leftarrow \gamma} = G. \quad (2)$$

At high energies, as $\gamma \rightarrow \infty$, $Q_E = Q_M = G\gamma$.

Note that the sign of Q_M is the same as the sign of G , which is positive for protons—proton spins precess more rapidly than their momenta in magnetic fields. Deuteron spins, with G negative, lag their momenta in magnetic fields.

In an electric field (such as the field of a nearby charged electrode or particle) with G_E positive, Q_E increases from -1 at zero velocity, eventually switching sign at the “magic” velocity where the spins in an all-electric ring are “frozen” (relative to the beam direction).

When a particle spin has precessed through 2π in the rest frame it has also completed one full revolution cycle from a laboratory point of view; so the spin-tune is a frame invariant quantity.

For p, p scattering we are not concerned with full turns in a magnetic storage ring; we are concerned with “partial turns” of one proton in the electric field of another—with the further complication that the “other” proton recoils. Roughly speaking though, in deflecting through an angular arc of, say, $2\pi/6$ the spin of a low energy particle in an electric field precesses relative to its momentum by $-\pi/3 = -60^\circ$.

G -values for most of the stable atomic nuclei in a few upper rows of the periodic table, plus tritium, which is weakly unstable, are given in Appendix A, along with other parameters. As mentioned previously, g and G are approximate rational ratios for convenience for their use in precision determination based on frequency domain determinations.⁴

2. T-violation and identical particle treatment

In a magnetic storage ring (possibly with weak electric bending superimposed) independently polarized bunches collide at the crossing point. Both initial proton polarization states are pure and some of the final state proton polarizations are measured with analyzing power close to 100%. Quantum mechanical predictions will be tested

⁴ For reasons that may or may not be physically significant, these G -values are also expressed as rational fractions, with the integer “6” favored, meaning that the denominator is either less than 7, or a multiple of 6. In some cases the rational values are smaller than the measurement errors; in most cases the rational fraction approximations are accurate to $\pm 1\%$ —good enough for semi-quantitative purposes, such as estimating the number of turns for a spin to return to its initial orientations. The number “6” is favored because the most favorable planar lattice is hexagonal for many purposes. Though this may be only of mystical significance, the rational fractions produce convenient answers.

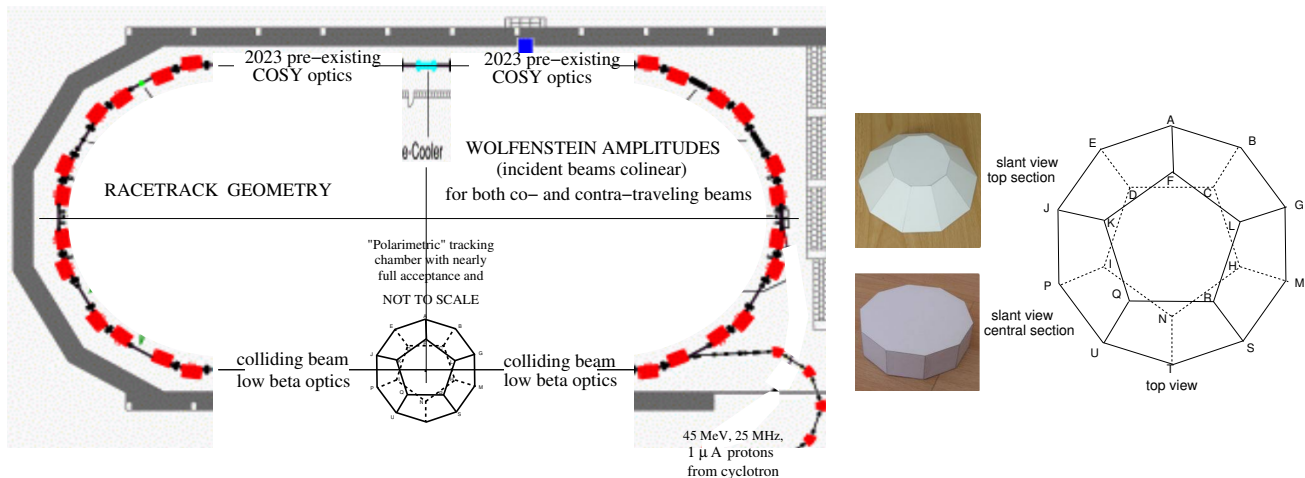


FIG. 3. This layout figure shows COSY (as of 2022) after incorporation of the superimposed electric bending shown in Figure 4. The semicircular arcs are preserved exactly as at present, except the arc magnets are powered individually, to compensate appropriately for the superimposed electric bending. “Co-traveling bunches” (needed for resonant nuclear transmutation) have same sign, parallel incident momenta. “Counter-traveling bunches” (needed for p, p scattering) also have parallel incidence momenta. **Right:** Artist’s conceptions of almost full-acceptance tracking/stopping/polarimeter chambers at the intersection point in the lower straight section. The top and bottom sections resemble partial Platonic dodecahedrons, with 12 identical planar faces, each subtending the same solid angle. Labeled vertices are for convenient reference here. For example, a “clean” stopping proton passing just below point F in the top pentagon can be expected to be in coincidence with a clean stopping proton midway between points C and D in the bottom pentagon. To accommodate passage of the colliding beams there can only be reduced particle detection in the central section.

by detecting correlation between the p -carbon measured spin orientations of final state protons.

Investigation of the influence of T-violation on p, p elastic scattering is emphasized in this paper. The combination of superimposed electric and magnetic bending and the measurement of final state polarizations enables the direct measurement of P- or T-violating amplitudes, which might very well have canceled in all previous experimental investigations of T-violation in p, p scattering.

The presence or absence of T-violation in nuclear forces is thought to bear significantly on important cosmological issues, especially missing mass, dark energy, and the matter/anti-matter imbalance. The possible existence of a semi-strong, T-violating, nuclear force with coupling strength comparable to the electromagnetic interaction was proposed independently by Lee and Wolfenstein[3], by Prentki and Veltman[4], and by Okun[5][6] in 1965.

Unlike fixed target experiments, rather than being collinear, in Derbenev[8] geometry, incident beams collide at right angles. Observed in the laboratory frame, all incident and elastic scattered energies are equal. It will be shown that this provides a huge statistical polarimetric advantage. *Persuasive visual evidence of T-violation will be provided by unexpected correlation between the polarimetric p -carbon scattering directions of final state protons.*

Spin dependence is most easily detectable at low proton energy. The proposed COSY lab rearrangement is a variant of PTR[10], a prototype EDM measurement ring. Rearrangement of existing COSY components into

a “FIGURE-8” storage ring allows diametrically opposite polarized proton bunches in a single stored beam to collide. “Derbenev spin transparency[11]” in figure-8 geometry is used to enable Fourier enhancement of T-violation sensitivity.

Of the uncertain properties of nuclear physics, none is more fundamental than nucleon, nucleon interaction, especially below pion production threshold. The Derbenev collider configuration enables measurement of “elastic” p, p scattering spin dependence not possible using fixed polarized hydrogen target. To be consistent with previous discussion, these events would be “prompt”.

This paper describes an experiment to investigate possible violation of time reversal invariance (T-violation) in “elastic” p, p scattering, where the quotation marks acknowledge the possibility of collisions for which the energy dissipation is undetectably small. This applies especially to below threshold (closed) resonant nuclear channels which would result in inelastic p, p scattering at higher energy but which, being below threshold energy, produce no new secondary particles. Above nuclear transmutation threshold energy (but below pion production threshold) these amplitudes promise substantial resonant room temperature storage ring nuclear transmutation. This is to be investigated in a separate paper.

Derbenev et al.[8] have produced a configuration enabling the investigation of scattering of orthogonal traveling protons at the crossing point of a figure-8 storage ring. A solitary stored beam “collides with itself” in the sense that diametrically-opposite bunches automatically

Large deflector tests

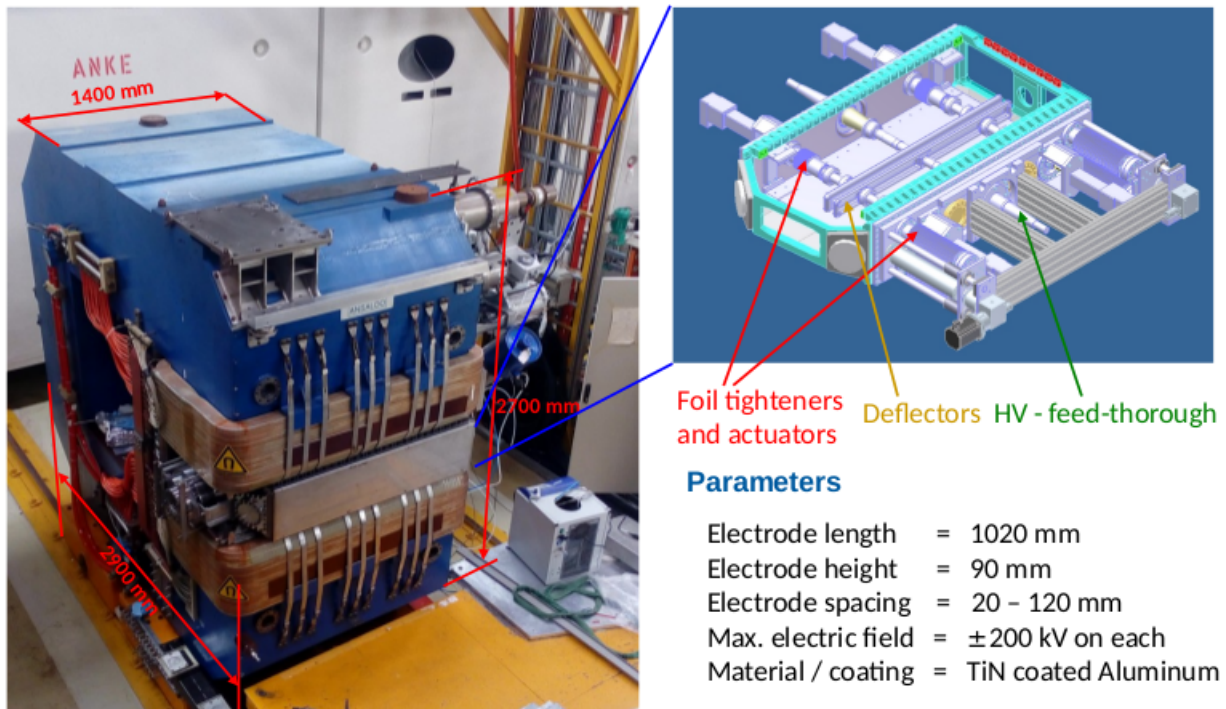


FIG. 4. Grigoryev prototype electric field insert in COSY bending magnets for 200 MeV (kinetic, laboratory) energy operation of COSY with electric bending superimposed on existing magnetic bending.

pass through each other in synchronism at the intersection point (IP) where the beam crosses itself.

There is a significant formal (but potentially qualitative) distinction between Wolfenstein and Derbenev geometry, closely correlated with the treatment of identical particles and with issues of distinguishing time priority and left/right scattering ambiguity. This ambiguity may correspond to a CM ambiguity noted by Ashtekar, De Lorenzo, and Khera[9]

In (collinear-incidence) Wolfenstein geometry, for exactly-parallel, but transversely separated by immeasurably small distance, it is impossible to associate final state left and right scatters with incident-state left/right orbit displacement. This is the source, in quantum mechanics, for treatment of identical particle scattering, to sum amplitudes over interchanged incident states, before calculating intensities.

In Derbenev geometry there is less ambiguity. A particle scattering promptly to the right must have come from the beam incident on the right, and vice versa. This is illustrated in Figure 9, to be discussed in more detail below. One notes, based on the ray tracing shown, that of the four possible final state angular quadrants, a

promptly scattered beam particle from the left, say west (W), may appear in the SW, NW, or NE quadrant, but be “captured” into a compound nucleus, preventing its prompt escape into the SE sector. This evolution would presumably proceed too quickly for scattering directions to be correlated with scattering times. Furthermore the time evolution description must be consistent for both scattered particles. Nevertheless, the evolution can be modeled theoretically, no matter how quickly it transpires, and the calculated distributions compared with experiment. It is only its spin state that can enable a particle to “remember” whether it came from the left or from the right, based on its theoretical evolution.

In the fullness of time such “resonant” states can be expected to produce more nearly isotropic, but stochastically distributed scattering directions, which classical mechanics cannot handle, even in principle, and quantum mechanics can handle only probabilistically. Since energy and momentum need to be conserved “in the long run” the time delay between prompt and delayed scatters may be immeasurable. One conjectures that this is controlled by entanglement of the final states and detectable only by measuring the correlation of final state spin ori-

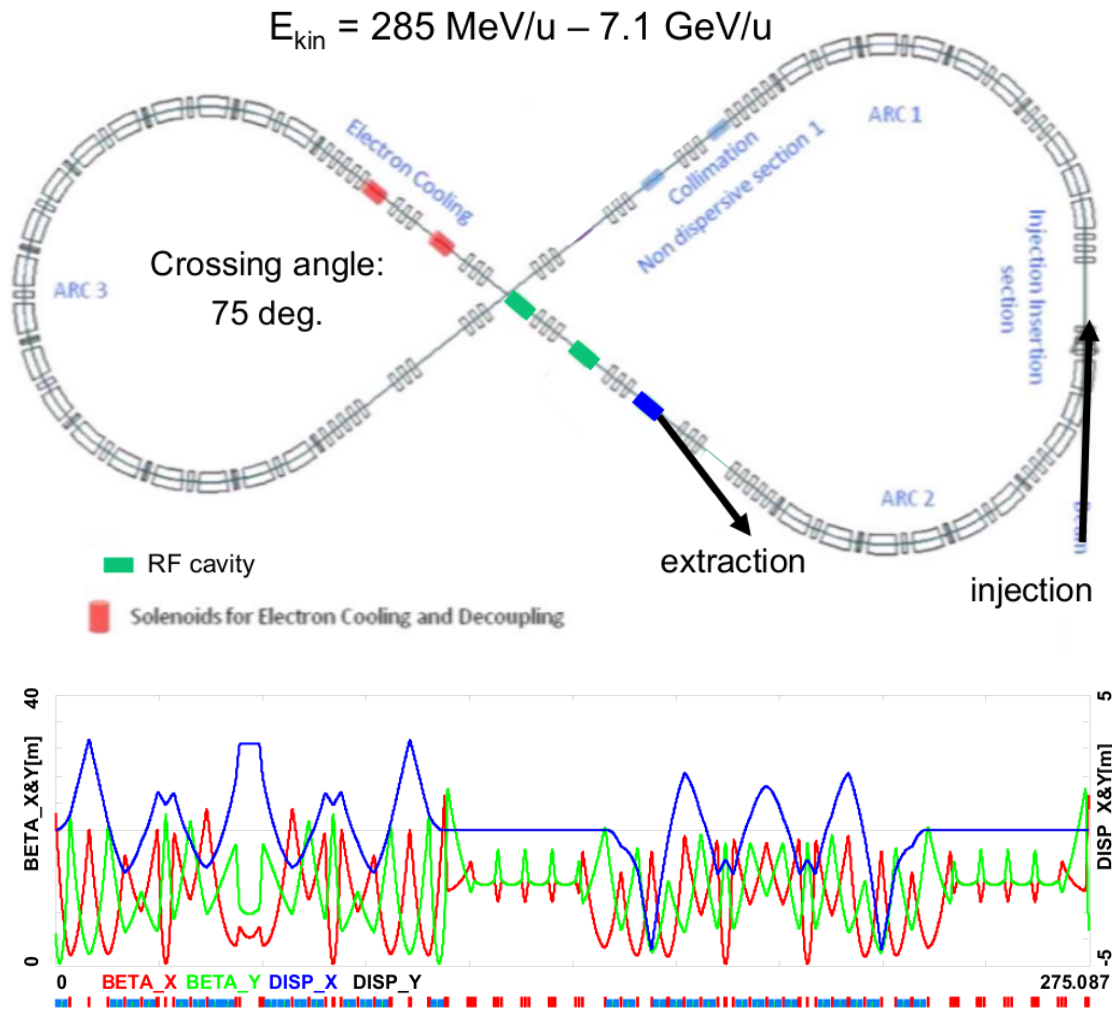


FIG. 5. These figures apply to the JLEIC-BOOSTER injector accelerator in the Jefferson Lab electron-ion collider, JLEIC injector line. Since this figure-eight ring has roughly the same size as the previously introduced COSY figure-8 ring, and serves comparable beam energies, the ring elements and lattice optics can be expected to be similar.

entations. Behavior during The delayed time interval is not essentially different from an electron being captured stochastically into eigenstates sorted by energy and angular momentum; except here it is stochastic decay into measurable final state protons.

For spin-1/2 particles, one conjectures that this distinction is correlated with the fact that in-plane (i.e. horizontal) deflections) preserve up or down states spin but mix horizontally polarized states. One also conjectures that these issues are correlated with rest-frame orientation ambiguity, which implicates the sub-group structure of inhomogeneous Lorentz groups. Otherwise it is difficult to reconcile incident (and outgoing) beam directions being orthogonal in the laboratory, yet collinear in the rest frame.

In Wolfenstein geometry this ambiguity is especially acute because the incident orbits are collinear. In Der-

benev geometry incident orbits can be coplanar but not collinear.

Accepting the Derbenev accelerator physics analysis of orbit and spin evolution, including “spin transparency”, a figure-8 storage ring having polarimetry with nearly full 4π acceptance, and analyzing power ranging from 80% to 100% over substantial solid angular range is described. Spin transparency enables a Fourier statistical enhancement of symmetry violation in p, p scattering.

3. Modern spin control; ancient nuclear physics

The energy region emphasized in this paper, “above” Rutherford scattering, “below” meson threshold, is paradoxical in various ways. Total p, p cross sections are discussed and plotted in detail in a heroic 1993 review

by Lechanoine-LeLuc and F. Lehar[14], containing seven pages of references, from an era in which a large experimental group had five members.

Figure 6 (copied from LeLuc and Lehar) shows measured elastic and inelastic p, p cross sections. Spin dependent p, p cross sections, measured with polarized beams and polarized hydrogen target are plotted at the bottom of Figure 6.

Though originally mysterious, the complicated long de Broglie wavelength behavior (i.e. low energy region below, say, 100 MeV) quickly became well understood in terms of interference between Rutherford and nuclear amplitudes. The same cannot be said for the short wavelength, higher energy region, above, say, 400 MeV, where inelastic scattering quickly becomes dominant.

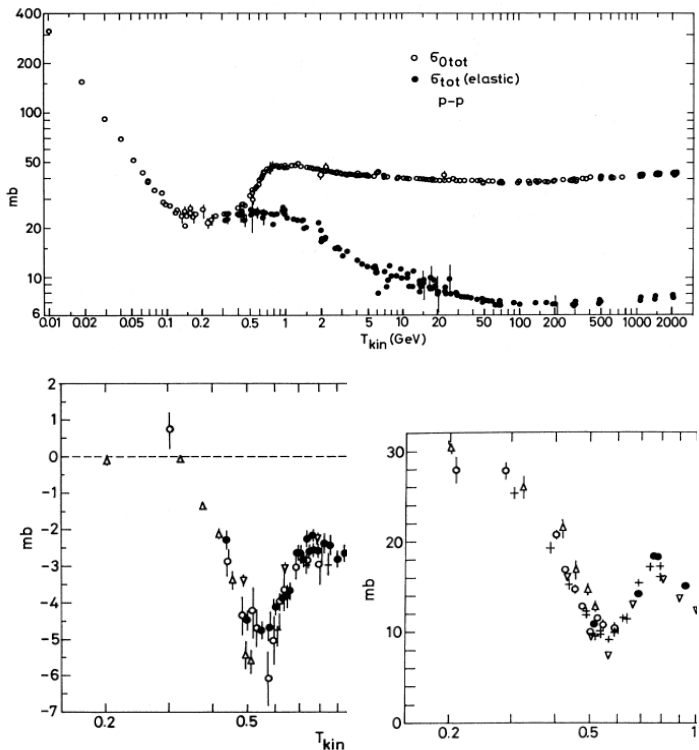


FIG. 6. (Copied from reference [14]) **Above:** Energy dependence of p, p spin-independent total cross section (open circles) and total elastic cross section (solid curves). **Below left:** $\sigma_{1tot}(p, p) = -(1/2)\Delta\sigma_T(p, p)$ energy dependence, **Below right:** $-\Delta\sigma_L(p, p)$ energy dependence on the incident state polarizations. This figure should be compared with Figure 8.

4. Conjectured “prompt” p, p scattering

From an experimentalist’s kinematic planning perspective p, p elastic scattering cross section in the 100 to 400 MeV energy range could scarcely be more boring—the scattering is isotropic and the total cross section is constant. It seems curious, therefore, that the error bars

and the scatter of values in this region are some five times greater than at almost any other region of the plot. Though not at all suggested by the upper plot, an empirical, partial wave fit at the center of the region, at 310 MeV, based on data available in 1965[15], required 12 non-vanishing partial waves, when the isotropy observed in coarse early experiments suggested that just one or two partial waves might be expected.

My picture has the variation through this intermediate energy range representing the transition from predominantly prompt, to primarily delayed, compound nucleus formation scattering probability, and ultimately to pion production, when the nuclear forces cannot handle the energy.

Of all nuclear processes it might initially have been expected that understanding elastic p, p scattering would be assigned highest priority. Based on counting citations, the number of PhD theses implied by the seven pages of reference[14], this effort was strongly supported for several decades. Yet, it seems fair to say that p, p elastic scattering is still not understood in any fundamental sense.

The plan is to improve this paradoxical history by better studying the influence of proton spins by improving the previously feeble experimental capability to control initial spin states and the previous inability to measure final state polarizations.

Since the angular momentum associated with the spins of fundamental particles is still mysterious, it should perhaps not be surprising that partial wave analysis, which is based on conservation of angular momentum remains purely phenomenological. The present proposal hopes to improve this situation.

Methods now available enable the preparation of pure initial spin states along with nearly ideal final state measurement of both final spin states over a significantly large fraction of available phase space. To be consistent with the huge investment in this area in the past one expects, therefore, significant support for these greatly improved methods in the present.

There is at least one exception to the statement made previously that p, p scattering is not understood in any fundamental sense.⁵ It is the so-called Gerasimov-Drell-Hearn sum rule[19][20], which connects static properties of the nucleon—like the anomalous magnetic moment and the nucleon mass—with an integration from zero to infinity, of a difference of spin dependent doubly polarized total absorption cross sections of real photons. Quoting from Helbing[21] “The experimental data verify the GDH Sum Rule for the proton at the level of 8% including the systematic uncertainties from extrapolations to unmeasured energy regions.” Based purely on sound field theory, this surely qualifies as “some kind of understanding

⁵ This GDH digression is the result of numerous conversations between the author and Kolya Nikoliev.

in a fundamental sense”.⁶

What may be hoped for from the GDH sum rule is better understanding of the paradoxical p, p interaction behavior under discussion. From a qualitative perspective, one anticipates an improved theoretical understanding of how cross sections well outside our narrow energy range can help to understand seemingly elementary elastic p, p scattering.

A paper by Bystricky, Lehar and Winternetz [22] provides a detailed breakdown of p, p and p, d scattering amplitudes, with special concentration on time reversal invariance (TRI). The paper by Lechanoine-LeLuc and Lehar[14], whose importance has already been emphasized, reviews the voluminous nucleon-nucleon elastic scattering data, including polarization, with analyses, as of 1993, from well below to well above the energy range considered in the present paper, up to a few GeV.

Vastly more powerful experimental tools are available today than in the past. This is especially true of the precision spin control techniques that have been developed at the COSY laboratory in Juelich Germany[23][24][25][26][27][28].

The exchange force, postulated initially by Heisenberg, later revised by Wigner and others, models the dependence on the same spins that control the polarizations of elastic nucleon scattering. Along with the importance of exchange forces in fitting the binding energies of all nuclei from $A=1$ to $A=200$, it was the assumption of time reversal (T) conservation that constrained this modeling. Then till now, other than its theoretical elegance, there has been no persuasive experimental evidence, one way or the other, for requiring T-conservation of the nuclear force.

With the anticipated EDM statistical precision inversely proportional to the square root of run duration in mind, it has, until recently, been assumed that polarized beam run duration times would be limited by the spin coherence time (SCT). Recent developments[29] have suggested that this will not be the case. Run durations in excess of 1000 s, (a conventionally-adopted design goal) are now thought to be allowed by lattice design optimized for the cancellation of sources of polarization decoherence.

A more important, and unavoidable, consideration limiting run durations, is now thought to come from the consumption of beam particles associated with the destructive polarization measurements needed for phase locking

the beam spin tunes[29]. This capability is needed to enable electric and magnetic fields to be repeatably set, reliably reversed and reset, without the need for (unachievably precise) electric and magnetic field measurement.

The ability to precisely reverse beam circulation directions provides powerful capability for reducing systematic error by averaging over beam revolution reversals. This has lowered the priority associated with requiring two beams to counter-circulate simultaneously rather than consecutively.

These considerations have motivated, in the present paper, the re-ordering of PTR prototype ring development sequencing from the ordering defined initially in the CERN Yellow Report (CYR)[10]. Development of the superimposed electric and magnetic sector bends needed for PTR can proceed “in parallel” with the construction of the FIGURE-8 ring and with the construction of the polarimetric tracking chamber needed for p, p scattering measurement, and applicable as well to EDM measurement; all with the common goal of investigating time reversal symmetry.

5. Investigation of the strong nuclear force

In 1950, when 20 MeV was “high energy physics”, nuclear EDMs were thought to play a significant role in the photo-disintegration of nuclei such as the deuteron. This physics is explained in Section XII-E of Morse and Feshbach[12]. The inferred value of the deuteron EDM at that time, as quoted by Gamow’s Table I[13], expressed as a photo-dissociation cross section was $2.7 \times 10^{-27} \text{ cm}^2$. The presence of what seems to be violation of time reversal (T) symmetry seems to have been forgotten. Perhaps Norman Ramsey’s surprise concerning a non-zero EDM effect provided some of his motivation for initiating his program to measure the neutron EDM? But subsequent measurements have provided only upper limits.

With co-author Kolya Nikolaev, a Snowmass 2021 presentation[30] describes how a ring such as described in the present paper can be used to investigate the possible existence of a beyond standard model (BSM) *semi-strong T-violation in elastic p, p or p, d scattering*.

In τ - θ puzzle days (late 50’s to mid-60’s) such a mechanism was suggested independently by Lee & Wolfenstein[3], by Prentki & Veltman[4], and by Okun[5][6][31]. Other, similarly motivated, conjectures have been numerous. Search for such a medium-strength, T-violating nuclear force provided the initial motivation for this paper.

The following few paragraphs have been extracted almost verbatim from Mott and Massey[15]

Especially influential were the “scalar” Wolfenstein operators, for primary beam particle “1” secondary target particle “2”;

$$\mathbf{1}, \quad \boldsymbol{\sigma}_1 \cdot \boldsymbol{\sigma}_2, \quad (\boldsymbol{\sigma}_1 + \boldsymbol{\sigma}_2) \cdot \mathbf{n}, \quad (\boldsymbol{\sigma}_1 - \boldsymbol{\sigma}_2) \cdot \mathbf{n},$$

⁶ As it happens, a peripheral capability of the apparatus we propose is the capability of precise measurement of MDMs of the nuclei of many low mass isotopes, stable or weakly unstable, to which other sum rules might apply. Since the proton MDM is already known to 11 decimal places, it cannot be claimed that this MDM capability is required to evaluate the right hand side of the GDH sum rule. Neither may it be claimed to very much improve the accuracy of the integrand on the left hand of the GDF formula.

$$(\boldsymbol{\sigma}_1 \cdot \mathbf{p})(\boldsymbol{\sigma}_2 \cdot \mathbf{p}), \quad (\boldsymbol{\sigma}_1 \cdot \mathbf{n})(\boldsymbol{\sigma}_2 \cdot \mathbf{n}), \quad (\boldsymbol{\sigma}_1 \cdot \mathbf{q})(\boldsymbol{\sigma}_2 \cdot \mathbf{q})$$

where “ $\mathbf{1}$ ” is the identity matrix, and the three components of the $\boldsymbol{\sigma}_1$ and $\boldsymbol{\sigma}_2$ “vectors” are the three Pauli 2x2 matrices. As shown in Fig. 7, orthonormal coordinate basis vector \mathbf{n} is an axial unit pseudo-vector which, with orthogonal incident momentum unit vectors \mathbf{p} and \mathbf{q} , defines the scattering plane, to which \mathbf{n} is orthogonal. These are the possible forms in terms of which the scattering matrix can be composed and matched phenomenologically with measured values at each value of beam energy.

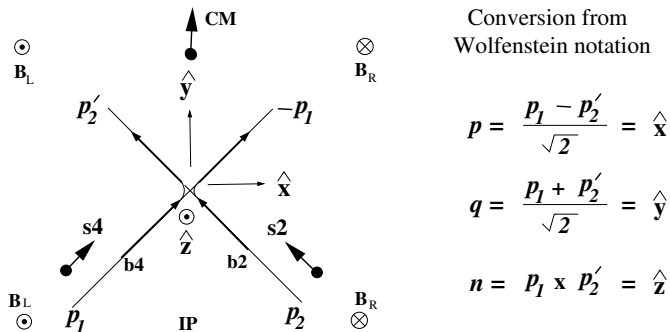


FIG. 7. For orthogonal beam collisions the Wolfenstein incident momentum unit vectors \mathbf{p} and \mathbf{q} , along with normal to the scattering plane $\mathbf{n} = \mathbf{p} \times \mathbf{q}$, become Cartesian unit vectors \hat{x} , \hat{y} , \hat{z} , in the transition from Wolfenstein to Derbenev configurations. The \mathbf{B}_L and \mathbf{B}_R symbols can only be understood in connection with Fig. 1.

Already formidably complicated, two Wolfenstein “pseudo-scalar” forms,

$$(\boldsymbol{\sigma}_1 \times \boldsymbol{\sigma}_2) \cdot \mathbf{n}, \quad \text{and} \quad (3)$$

$$(\boldsymbol{\sigma}_1 \cdot \mathbf{p})(\boldsymbol{\sigma}_2 \cdot \mathbf{q}) + (\boldsymbol{\sigma}_1 \cdot \mathbf{q})(\boldsymbol{\sigma}_2 \cdot \mathbf{p}) \quad (4)$$

have (conventionally) been excluded on the basis that they violate T-reversal and/or P-symmetry. An intermediate strength T- or P-violating nuclear force can be represented by a superposition of operators 3 and 4.

Based on this phenomenological formulation, a description of nuclear forces capable of accurately accounting for the parameters of all nuclei and of accounting for the decay of all unstable nuclear isotopes was gradually established. A substantial portion of this understanding was based on the treatment of protons as elementary particles for which there was no relevant concept of “binding energy” required. Binding energies were defined relative to the proton binding energy (taken to be zero). In detail, the exchange force was taken to be a best compromise of Heisenberg, Wigner and Majorana exchange force variants, based on measured binding energies.

By τ - θ puzzle days, the elementary particle community had “moved on” from what had by then become “low energy” nuclear physics, accepting, with little subsequent

alteration, the existing phenomenologic description of the force between nucleons. Note, however, that there has been little other than theoretical prejudice for requiring time reversal symmetry conservation.

In the meantime, Gell-Mann quarks had been introduced as constituents of the proton. This made protons composite, contrary to already adopted modeling that treats the proton as elementary. Logically, its composite nature might reasonably have been accompanied by the possibility of the proton itself having binding energy⁷.

There is thought to be a close connection between time reversal (T-symmetry) and the baryon/anti-baryon imbalance in our present day universe. This connection was stressed by Sakharov[33] in an early and influential paper. Nowadays, to a first approximation, our universe contains only protons. One has to suppose that the laws of particle physics are consistent with symmetry-breaking processes which have resulted in a surplus of what we now call protons. As Sakharov famously explained, any generation of such an imbalance of particles and anti-particles required statistical disequilibrium conditions, absence of baryon number conservation, and CP- (and hence also T-) violation in one or more of the fundamental laws of particle production and decay.

Building on the Wolfenstein formulation, traditional analyses, after having dropped the T-violating operators, have proceeded to simplify the algebra by proceeding to a density matrix formulation. This approach assumes implicitly that every experimental elastic scattering apparatus is limited in a way that, for identical particles, requires averaging over incident states and/or summing over final state amplitudes with interchanged output directions. Here it is argued that the summing of amplitudes with interchanged output directions is not appropriate in Derbenev geometry, since, for the majority of them, it is possible to match each promptly scattered proton with the incident beam, left or right, that it came from.

The fact that the Pauli operators are 2x2 matrices makes it difficult to acquire any simple intuitive correlation between momenta, on the one hand, and separation into spin-flip and non-spin-flip events on the other. Density matrix formulation makes this algebraically convenient. This is even true when both incident states are pure, as we are assuming. Mott and Massey[15], Section IX.5, explain this in detail. It is useful to employ spherical coordinates with in-plane cylindrical polar angle θ and out of plane azimuthal ϕ coordinates.

For the detection apparatus proposed here there is no need for the summing or averaging of amplitudes. The explicit isolation of symmetry-violating and symmetry-conserving amplitudes makes the basic Wolfenstein for-

⁷ In a paper introducing integer charge quarks, Han and Nambu[32] suggested implicitly the influence on binding energies, but, with “color” persuasively introduced, this seems not to have been pursued.

mulation seem appropriate. However, the Derbenev geometry also avoids the need for averaging over final states to account for identical incident particle types. Clearly, in an actual elastic nuclear scatter, each strongly scattered proton counts in the sector at which it *was not previously aimed*.

The Wolfenstein configuration suffers from the essential singularity appearing at the center of phase space which makes particle interchanged summation necessary. In the Derbenev configuration this identical particle singularity appears harmlessly in the form of weakly scattered proton directions centered on the forward direction but with large impact parameters approaching the boundary of phase space.

6. Importance of anomalous nuclear MDM G -values

The motivation for the storage ring or (or rings) being promoted in this paper centers on the careful study of “elastic” nucleon scattering. The guiding rationale emphasizes the important role played by the anomalous MDM, G , in elastic nucleon scattering. An essential feature of the rings being advocated here follows from their superimposed electric and magnetic bending, which provides the capability of simultaneously counter-circulating frozen spin beams of different particle type.

As explained in publications [1] and [2], this storage ring configuration is ideal for the precision measurement of anomalous nuclear MDM G -values. Such rings serve naturally for the function of “mutual co-magnetometry” for precise measurement of the ratios of the numerator and denominator integers entering into the precision experimental determination of G -values of the particle types in the two counter-circulating beams.

For historical reasons, based probably on the great importance and successful application of the g -factor in atomic physics, the (dimensionless) parameter G is considered to be subsidiary to the (also dimensionless) “ g -factor”, which expresses (in our nuclear case) a fundamental measurable ratio of nucleus angular momentum (proportional to inertial mass m of nucleon) to magnetic moment (proportional to charge of the same nucleus).

With Z and A being dimensionless measures, the ratio of integers, A/Z , justifies regarding $g(A/Z)$ as function A and Z only via the ratio A/Z . To be “anomalous” the dimensionality of G and g must be the same: i.e. dimensionless.

For every nucleon, Z is truly an integer multiple of (positive) proton charge e . Regrettably, for example because of nuclear binding energy, nucleon mass ratio is only only approximately given by the mass number A .

This discussion is continued in Appendix A, but not because it is of lesser importance; in fact this paper provides further strong support for the precise measurement, and consistency treatment of nuclear isotope MDMs and mass values. But the discussion is both technical and

boring. This justifies treating Appendix A as a self-contained discussion of the experimental and theoretical connections between g and G [16][17].

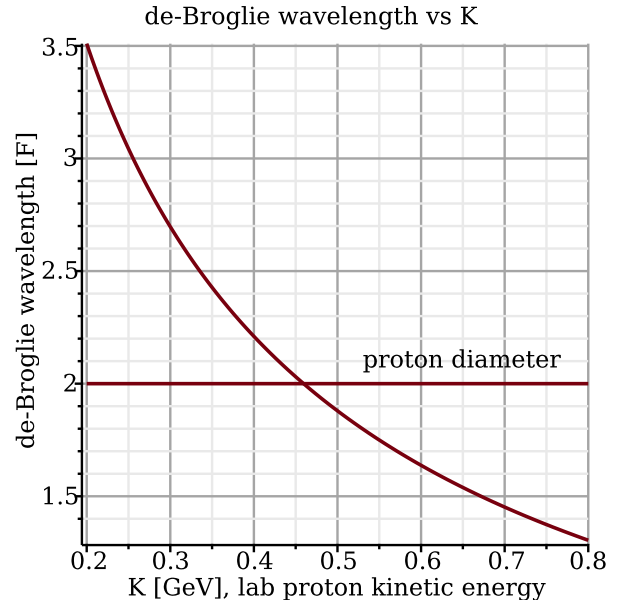


FIG. 8. Fermi length units plot of the deBroglie wavelength of an incident proton versus its total laboratory kinetic energy. See Appendix Section A 1, for numerical values of various nuclear parameters. The approximate match of deBroglie wavelength with proton size can scarcely be simple coincidence. Surely this represents a nominal transition point from wave to particle description of p, p scattering; much like the transition from geometric to wave optics. New “particles” need to be massive, in this case pi-mesons, to account for the available energy, while conserving momentum at the local velocity. Azimuthal symmetry is broken on an event by event basis, but is, presumably, preserved on average. For correlation with, say, rainbows, refer to Van-de-Hulst[18]; a further empirical numerical factor, $\pi(m - 1)$ of order 1, multiplying the diameter, is required, where m is “index of refraction”.

IV. ORTHOGONAL COLLISIONS OF PAIRED BUNCHES IN A SINGLE BEAM FIGURE-EIGHT STORAGE RING

1. Wolfenstein/Derbenev amplitude comparison

During the infancy of nuclear physics all possible experiments were “fixed target”, with kinematically unbalanced initial states; with special relativity still controversial, “energy” meant kinetic energy (K), which, by convention, was used to label energy dependent data. A century later, using Derbenev figure-eight geometry, we are in a position to perform the same definitive experiments with symmetric incident states.

Before continuing, it has to be recognized that what has been referred to as WOLFENSTEIN configuration has been specific in meaning “collinear incident

beams”, but ambiguous as to frames of reference. Before the advent of storage rings the incident beam passed through a target fixed in the “laboratory frame”, where unprimed kinematic parameters are employed. In the center of mass system, whose parameters are distinguished from corresponding laboratory frame by the attachment of a single prime. Though the centroid moves in the laboratory, it stays on the original beam line and the centroid of every scatter starts on, and remains on, the same stationary beam line.

Nowadays, for high energy circular collinear (Wolfenstein) colliding beam storage rings, mechanical energy $\mathcal{E} = mc^2 + K$ is used to specify incident beam energies. This labeling is ideal, since the center of mass (CM) and laboratory frames are identical. But, for Derbenev beam self-collision the CM and laboratory frames are different. (The same is true for collisions between countercircling in rings with superimposed electric and magnetic bending.) For meaningful comparison of D&W physics results it is useful to introduce a “comparison energy” $M^* = \sqrt{s}$, which, in every case, is the total mass of the p, p system in the CM reference frame. The natural data comparison then is between data sets for which

$$M^* = \sqrt{s} = M_W^* = M_D^*.$$

Laboratory frame descriptions are convenient for both W and D configurations. This makes it sensible to perform all kinematic calculations in the laboratory before equating their determinations of M^* which (with $c = 1$) is the rest energy in the CM frame. All other kinematic variables refer implicitly to the lab frame. Avoiding kinetic energy (until the end) and never evaluating square roots, avoids the need ever to solve a quadratic equation.

With “W” subscripts, the square of the total energy in collinear Wolfenstein fixed target laboratory frame configuration, with $c = 1$ and total energy squared $\mathcal{E}_{\text{tot.-W}}^2$, and with proton mass m , is given by

$$\mathcal{E}_{\text{tot.-W}}^2 = (\mathcal{E}_W + m)^2 = \mathcal{E}_W^2 + 2m\mathcal{E}_W + m^2. \quad (5)$$

Total momentum and CM rest mass are then given by

$$\begin{aligned} p_{\text{tot.-W}}^2 &= p_W^2, \quad \text{and} \\ M_W^{*2} &= \mathcal{E}_{\text{tot.-W}}^2 - p_{\text{tot.-W}}^2 \\ &= \mathcal{E}_W^2 + 2m\mathcal{E}_W + m^2 - p_W^2 \\ &= 2m\mathcal{E}_W + 2m^3. \end{aligned} \quad (6)$$

In Derbenev figure-8 configuration,

$$\begin{aligned} \mathcal{E}_{\text{tot.-D}}^2 &= (2\mathcal{E}_D)^2 = 4\mathcal{E}_D^2, \\ p_{\text{tot.-D}}^2 &= \left(2\frac{p_D}{\sqrt{2}}\right)^2 = 2p_D^2, \\ M_D^{*2} &= \mathcal{E}_{\text{tot.-D}}^2 - p_{\text{tot.-D}}^2 \\ &= 4\mathcal{E}_D^2 - 2p_D^2 \\ &= 2\mathcal{E}_D^2 + 2m^2. \end{aligned} \quad (7)$$

Equating centroid rest energies produces

$$\mathcal{E}_D^2 = m\mathcal{E}_W \quad (8)$$

The purpose for this calculation has been to determine, in Derbenev configuration, the “ring energy”, \mathcal{E}_D , that corresponds to the Wolfenstein configuration “laboratory energy”, K_W , in terms of which historical experimental data is still recorded and referenced. (This resembles the historical nuisance task needed to transform angular distributions measured using targets fixed in the laboratory, to center of mass angles.)

Finally, to complete this task, requires relating K_W , the “historical kinetic energy”⁸ to “modern day mechanical energy”, \mathcal{E}_D ;

$$\mathcal{E}_D^2 = m(m + K_W). \quad (9)$$

This relation is troubling from both mathematical and quantum mechanical perspectives. With m treated as necessarily real, the limiting behavior of \mathcal{E}_D and K_W , individually treated as analytic functions of m , the square root required in the transformation becomes mathematically problematic as $m \rightarrow 0$.

From a quantum wave mechanical perspective, the issue is more confusing, especially with respect to de-Broglie relations for momentum and energy,

$$p = h/\lambda, \quad E = h\nu,$$

with all quantities in these relations required to be real.⁹

For the 183.1 MeV central energy of the Derbenev ring proposed in the present paper, the kinetic energy is obtained as;

$$\begin{aligned} K_W &= (m + K_D)^2/m - m, \\ &\underline{\underline{e.g.}} \quad \frac{(0.938 + 0.183)^2}{0.938} - 0.938 = 0.402 \text{ GeV}, \end{aligned} \quad (10)$$

which is appropriate for the horizontal axis scales in Figure 6. Since the energies are only weakly relativistic, the Derbenev kinetic energies are roughly half the Wolfenstein kinetic energy.

The proposed figure-8 storage ring is shown schematically in Figures 1 and 2. Though intended to serve as a measurement of elastic scattering, the experiment commences by treating the apparatus as two matched polarimeters being “calibrated” in coincidence. A single

⁸ Historically, K_W was expressed simply as “particle energy”.
⁹ The appearance of the symbol “i” as an abbreviation for $\sqrt{-1}$ enters QM formulas both for *trivial convenience* in the expression of trigonometric identities, and for *deep physics reasons* such as expressing the resonant build-up or exponential-decay of physical states. Strictly speaking, it is not logically required for just one symbol to play both of these roles. However this suspect symbolic usage is hopelessly entangled (pun intended) in customary treatments and understanding of quantum mechanics, including the present paper.

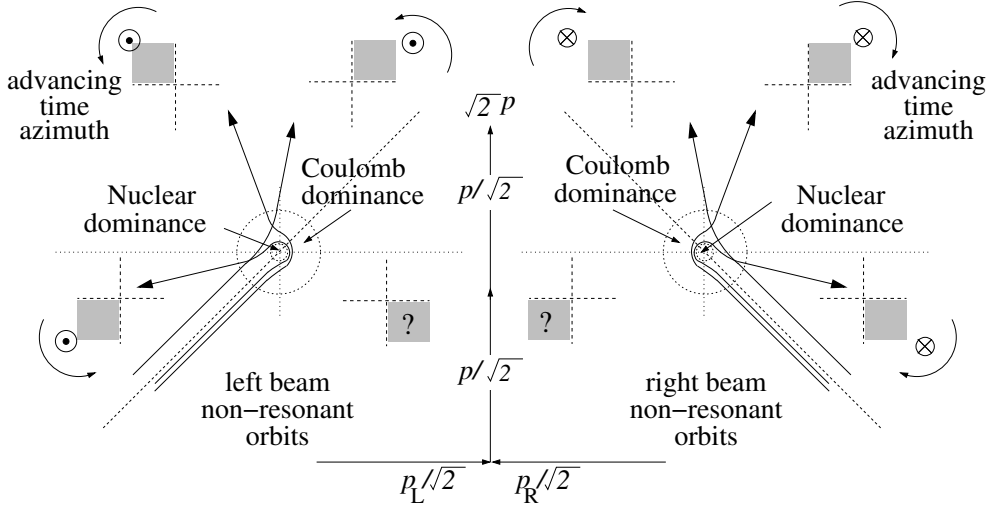


FIG. 9. "Prompt" classical orbits (or wave eikonal curves) representing a sequence of three particles (or wave packets) sequentially following the mutual scattering of a pair of protons, one from each beam, one into each of three azimuthally (i.e. "in a periodic angular sense") advancing sectors. By the fourth sector it has become ambiguous (classically) or probabilistic (quantum mechanically) whether the particle is detectable immediately or has been "mutually captured" by the other nucleus. Semicircular arrows indicate the sense of azimuthal advance (which is necessarily opposite opposite for the two scattering particles). The epoch represented begins just before and ends just after the actual collision. Inset graphs show horizontal plane quadrants, viewed (for example) from above. The shadings represent the sequencing of events, by indicating the quadrants in which successive events terminate. Individual orbits can be labeled by "azimuthal time", with one "typical" prompt orbit shown in each of the first three quadrants after the collision. As regards Newtonian particle description this represents the "complete story"—the subsequent evolution is unpredictable in principle. As regards "quantum wave physics" the figure represents evolution only up to the end of an initial time interval—the subsequent evolution is predictable in principle, but only in a statistical sense—for example, the fourth scatter may, or may not, result in an event in the fourth quadrant. Calculation of the subsequent probabilities requires quantum mechanics, and is limited by the Heisenberg (time) uncertainty; or (equivalently) by limitations imposed by mathematical properties of the Fourier transforms used to calculate the probabilities.

beam contains four bunches, \mathbf{b}_1 , \mathbf{b}_2 , \mathbf{b}_3 , and \mathbf{b}_4 , with individually controlled polarizations \mathbf{s}_1 , \mathbf{s}_2 , \mathbf{s}_3 , and \mathbf{s}_4 . Fig. 1 shows bunches \mathbf{b}_2 , and \mathbf{b}_4 about to collide at the intersection point (IP).

It is implicit in the Wolfenstein operator definitions for the incident beams to be collinear. In our application the incident beams are orthogonal in the laboratory reference frame, even though they are collinear in the CM frame, (which is shown moving upward in Fig. 7). Our configuration, which resembles Wolfenstein's t -channel, is shown with time advancing directly up the page.

The CM velocity is not very large in the laboratory, and significant CM symmetry is preserved because of the transversely symmetric orthogonal approach of the incident beams in the laboratory. Though the protons approach at right angles in the lab, in the CM frame the approach is collinear, as are the scattered trajectories.

The corresponding laboratory frame constraint is that incident and scattered momenta pairs are orthogonal, and all four energies are identical. In the laboratory, as well as defining a (horizontal) plane, the incident trajectories define a $\pm\pi/4$ "right-angle cone", centered on the transverse axis along which the CM is traveling. The scattered trajectories necessarily lie on the other branch of the same cone, necessarily orthogonal also, and defin-

ing a plane containing the same conical axis but, in general, skew to the horizontal plane, by some non-zero azimuthal angle Φ .

With the incident particle momenta defining a circle on the cone of incidence, the scattered particle momenta lie on the mirror-symmetric circle on the other branch of the cone. As a consequence, the scattered particle trajectories are also orthogonal in the laboratory with identical energies, the same as the incident particle energies. *It is their equal energies that permit both scattered particle polarizations to be measured with nearly perfect 100% analyzing powers.*

Wolfenstein's incident particle momenta are \mathbf{p}_1 and \mathbf{p}_2 , and scattered particle momenta are \mathbf{p}'_1 and \mathbf{p}'_2 . Our incident particles \mathbf{p}_1 and \mathbf{p}_2 are his \mathbf{p}_1 and $-\mathbf{p}_2$. Fig. 7 includes translation formulas on the right for conversion back to Wolfenstein's basis vector definitions.

So far it is only the \mathbf{b}_2 , \mathbf{b}_4 bunch pairing that has been discussed. Of course, the same discussion applies to the \mathbf{b}_1 , \mathbf{b}_3 bunch pairing. During bunch polarization preparation each of the four bunch polarizations can be prepared arbitrarily. This makes it convenient to compare the different outcomes from differently prepared incident states merely by maintaining the separation of "even bunch index" and "odd bunch index" incident bunch

pairs.

V. PAIRED BUNCH COLLISIONS IN ELECTRIC/MAGNETIC STORAGE RINGS

1. Superimposed magnetic/electric bending

During the infancy of nuclear physics all possible experiments were “fixed target”, with kinematically unbalanced initial states; with special relativity still controversial, “energy” meant kinetic energy (K), which, by convention, was used to label energy dependent data. A century later, using superimposed electric and magnetic bending, we are in a position to perform the same definitive experiments with symmetric incident states.

Nowadays, for high energy circular colliding beam storage rings, mechanical energy $\mathcal{E} = mc^2 + K$ is used for incident beam energies. This labeling is ideal, since the center of mass (CM) and laboratory frames are identical. But, for scattering in the CM, but particle detection in the laboratory the frames are different. For meaningful kinematic comparison it is useful to introduce as “comparison energy” $M^* = \sqrt{s}$, which is the total mass of the p, p system in the CM reference frame.

The proposed figure-8 storage ring is shown schematically in Figures 1 and 2. Though intended to serve as a measurement of elastic scattering, the experiment commences by treating the apparatus as two matched polarimeters being “calibrated” in coincidence. A single beam contains four bunches, \mathbf{b}_1 , \mathbf{b}_2 , \mathbf{b}_3 , and \mathbf{b}_4 , with individually controlled polarizations \mathbf{s}_1 , \mathbf{s}_2 , \mathbf{s}_3 , and \mathbf{s}_4 . Fig. 1 shows bunches \mathbf{b}_2 , and \mathbf{b}_4 about to collide at the intersection point (IP).

It is implicit in the Wolfenstein operator definitions for the incident beams to be collinear. In our application the incident beams are orthogonal in the laboratory reference frame, even though they are collinear in the CM frame, (which is shown moving upward in Fig. 7). Our configuration, which resembles Wolfenstein’s t -channel, is shown with time advancing directly up the page.

The CM velocity is not very large in the laboratory, and significant CM symmetry is preserved because of the transversely symmetric orthogonal approach of the incident beams in the laboratory. Though the protons approach at right angles in the lab, in the CM frame the approach is collinear, as are the scattered trajectories.

The corresponding laboratory frame constraint is that incident and scattered momenta pairs are orthogonal, and all four energies are identical. In the laboratory, as well as defining a (horizontal) plane, the incident trajectories define a $\pm\pi/4$ “right-angle cone”, centered on the transverse axis along which the CM is traveling. The scattered trajectories necessarily lie on the other branch of the same cone, necessarily orthogonal also, and defining a plane containing the same conical axis but, in general, skew to the horizontal plane, by some non-zero azimuthal angle Φ .

With the incident particle momenta defining a circle on the cone of incidence, the scattered particle momenta lie on the mirror-symmetric circle on the other branch of the cone. As a consequence, the scattered particle trajectories are also orthogonal in the laboratory with identical energies, the same as the incident particle energies. *It is their equal energies that permit both scattered particle polarizations to be measured with nearly perfect 100% analyzing powers.*

Wolfenstein’s incident particle momenta are \mathbf{p}_1 and \mathbf{p}_2 , and scattered particle momenta are \mathbf{p}'_1 and \mathbf{p}'_2 . Our incident particles \mathbf{p}_1 and \mathbf{p}_2 are his \mathbf{p}_1 and $-\mathbf{p}'_2$. Fig. 7 includes translation formulas on the right for conversion back to Wolfenstein’s basis vector definitions.

So far it is only the $\mathbf{b}_2, \mathbf{b}_4$ bunch pairing that has been discussed. Of course, the same discussion applies to the $\mathbf{b}_1, \mathbf{b}_3$ bunch pairing. During bunch polarization preparation each of the four bunch polarizations can be prepared arbitrarily. This makes it convenient to compare the different outcomes from differently prepared incident states merely by maintaining the separation of “even bunch index” and “odd bunch index” incident bunch pairs.

2. Near perfect analyzing power

Nearly perfect analyzing power is less impressive (but no less essential) than it seems. As a proton slows down, its analyzing power exceeds 0.99 only briefly. However the analyzing power remains greater than, say, 0.8 for an appreciable fraction of the proton’s full range. Since the scattered proton energies are identical in the laboratory, the beam energy does not need to be much greater than 183.1 MeV, for all scattered energies to exceed the energy at which the graphite analyzing power exceeds 99%. Also graphite chamber thickness great enough to stop all scatters is easily achieved, irrespective of scattering angle. See Fig. 10 and Table II.

The polarization of every proton scattered at the IP, and scattered again in one of the near crystalline graphite foil (or construction grade graphene) plates of the detection chamber, will have been determined with unprecedented accuracy, irrespective of scattered proton direction. This will provide high quality positive elastic signature for every elastic scatter. The total stopping ranges of most protons, including weakly inelastic scatters, will be used to reject inelastic scatters.

With such cleanly matched pairs of elastic scatters, the comparison of time-forward and (effectively) time-reversed scatters can be performed with unprecedented accuracy on an event by event basis. For example, the equality of scattering probability P and analyzing power A (required to be equal by time reversal symmetry) can be checked for matched pairs of protons. Furthermore, (with sufficient incident spin orientation control) by altering the incident pure polarization states, the reversed-time version of any observed forward-time scatter can

be re-created. In other words, truly forward-time and backward-time scatters can be compared.

VI. LOW ENERGY p,p ELASTIC SCATTERING SEARCH FOR TIME-REVERSAL VIOLATION

1. Detection apparatus

The goal of the proposed scattering experiment is to reduce, by a large factor, elastic scattering p,p T-violating upper limits, currently roughly one percent. This would use highly polarized beams in the figure-eight storage ring being described in the present paper for colliding beam elastic scattering measurement. Even though some electric bending will eventually be required for EDM measurement using PTR, initially the bending will be all-magnetic.

Magnetic fields are opposite in the two partial rings making up the figure-eight bending. Counter-circulating beams are not required. Diametrically opposite bunches, such as **b2** and **b4**, collide at intersection point IP, at the center of the cross-over line.

An important role of RF acceleration (which is not shown, and which necessarily averages to zero) is to phase lock the beam revolution frequency to an extremely accurate absolute frequency over long runs. A possibly more important role is one which will require the quite high RF frequency required to prepare the short bunch lengths that will be needed to achieve high luminosity. If there is an “Achilles’s’ heel” to the present proposal, this is it.

The plan is to measure below-pion-threshold elastic p,p (or d,d) scattering in (fixed-target-equivalent) $100 < E < 400$ MeV laboratory energy range. This would exploit the JEDI-Juelich-developed [10] long spin coherence time, spin phase-locked, pure spin-state, polarized beam technology.

Final-state, single-particle polarization measurements are sensitive to T -violation in double-spin observables. For the goal of detecting T -violation in (measurably) elastic p,p (or d,d) scattering, the detection chamber shown on the right in Fig. 3 is located at the intersection point (IP) of the figure-8 ring.

The proposed tracking chambers are up-down (or left-right as appropriate) symmetric, with nearly full 4π solid angle detection, except for the vertically-central section which is heavily compromised by the requirement that the colliding beams are crossing at right angles.

Final state detection will be provided for nearly every elastic p,p scatter, by stopping both scattered particles in coincidence in the up-down (or left-right) symmetric, polarization-sensitive, tracking chambers. With nearly full acceptance, high-efficiency polarimetry is provided for every elastic p,p scatter.

Description of this capability is especially simple since, unlike scattering from a target fixed in the laboratory, the storage ring frame of reference is close to the CM frame. The negligible spread of stopping energies makes

it practical to study the full stopping tracks of both scattered particles for every scatter. This “clean” scattering detection provides a substantial advantage for colliding beam measurement compared to fixed target measurement. Here “clean” particle detection means two unambiguous single tracks detected in time-coincidence, with accurately valid kinematics. Final state proton energies will be equal, which can be expected to provide sensitive elastic/inelastic selectivity. These events will provide accurate spin-dependent differential cross section measurements over most of 4π steradians.

2. Luminosity estimation

Colliding beam luminosity and collision rate estimates have been performed. Based, as they are, on luminosity formulas that apply to head-on collisions, these formulas undoubtedly over-estimate the luminosity of right angle collisions. From this perspective, our assumed data rates are over-estimates. *Until realistic transfer line optics and realistic longitudinal beam dynamics has been established, the absolute rates used in this paper are not very reliable.* One can say, alternatively, that the run durations required to obtain the assumed numbers of scattering events is uncertain.

3. Data rate estimation

Other rate considerations are also important. As well as enabling high beam polarizations, electron cooling inherited from COSY will reduce beam emittances, and energy spreads. From this perspective, our assumed rates are under-estimates.

With roughly one in 400 tracks scattering elastically in a carbon polarimetry tracking chamber, 10^6 events are expected to exhibit at least one elastic p -carbon scatter. With both incident beams being, say, nearly 100% up-polarized, these million events would be candidates for potential detection of spin flips forbidden by T -symmetry. These are favorable events in the sense that a substantial fraction are subject to polarimetric analyzing power averaging greater than, say, 80%.

Persuasive visualization of T -violation will be provided by unexpected correlation between the azimuthal scattering directions of coincident final state protons upon their entry to the tracking chambers, where the analyzing powers are close to 100%. When all events are distributed by their (precisely-known) energies, their distributions in energy must match the dependence of analyzing power on energy, which is close to 100% for tracks starting close to the entrance to the detection chamber. As a result the events carrying most of the statistical information are the “early scatters” occurring shortly after chamber entrance. This makes it sensible to tally up-down and

left-right polarization determinations layer by layer in the tracking chambers. In other words, efficiencies and analyzing powers can be evaluated layer by layer, with events sorted into corresponding bins.

Of the 10^6 events just discussed, roughly 2500 will show two clean polarization sensitive scatters. Events with both tracks showing carbon scatters close to the chamber entrance will be “gold-plated” in the sense that both scattered particle spin states have been measured with high analyzing power, meaning that their spin state, “up” or “down” is known with near certainty. Of course, these will represent only a quite small fraction of the double-scatter events, but their statistical weight will be huge.

So far the distributions have been assumed to contain no T-violating scatters. One sees, already, the need for quite complicated data processing, in order to identify T-violating events. One therefore seeks initial spin state preparation that can be expected to maximize the fraction of events that are good candidates for counting as evidence of T- or P-violation¹⁰.

Investigation to be spelled out next, has produced the initial spin state preparation shown in Fig. 11.

4. Forbidden “null detection” of T-violation

Because of CPT symmetry, which is usually assumed to be sacrosanct, a violation of CP-symmetry is equivalent to a violation of T-symmetry. Though CP violation of the weak nuclear force has been observed, this violation seems too weak to account for the imbalance of matter and anti-matter in the present day universe. Current models have both strong interaction and electromagnetic interactions preserving P and T symmetry individually. Since charge conjugation plays no role in elastic nuclear scattering, CPT-conservation reduces to PT violation for nuclear scattering, such as the elastic p, p or d, d scattering under discussion. This does not make the detection of P-violation and T-violation equivalent, however, for various reasons.

Though weak (by definition) the weak nuclear force can be expected to play some role in elastic p, p or d, d scattering. So the detection of P-violation, *per se*, would be of less interest than the detection of T-violation. More important, and considered next, is the fact that there are significant theory-based limitations to the extraction of T-violation from experimental measurement of scattering rates.

This issue was introduced by Arash, Moravcsik and Goldstein[34] who showed that, independent of dynamical assumptions, no “null T-violation experiment” could

be designed. Here a “null experiment” experiment is defined to mean any experiment for which a statistically significant non-vanishing observed counting rate would demonstrate time reversal violation.

Before commencing their proof, these authors usefully define three classes of symmetry-violation detection experiment: (i) performing sequentially, an experiment followed by “theoretically the same” experiment run backwards in time; (ii) measuring a “self-conjugate” reaction which, under time reversal, goes into the same reaction; and (iii) a null experiment, as defined in the previous paragraph. The authors cite experiments of type (iii) that set fractional upper limits on parity-violation as small as 10^{-7} . The simplest example of type (i) is the time-reversal scattering requirement for polarization P in a forward scattering process to be equal to analyzing power A in the time-reversed process.

Arash et al. point out the necessity of significantly different apparatus for type (i) counting rate comparisons, and (correctly, from this experimentalist’s point of view) of an inevitable uncertainty in matching the acceptance apertures of two diverse experiments to an accuracy very much better than 1 percent. It becomes increasingly difficult to reduce violation upper limits by an increasingly large factor.

Arash et al. proceed to prove the impossibility of designing a null experiment capable of detecting T-violation. Taken together, their arguments present a bleak future for direct experimental detection of T-violation. This section reviews the Arash et al. results. A later section describes the extent to which our proposed storage ring experiment circumvents some of their detailed conclusions without contradicting their acknowledged validity.

A predicate for the Arash, Moravcsik and Goldstein (mathematically abstract) proof is that measurable polarized state scattering rates are due exclusively to bilinear combinations of scattering amplitudes. They do, however, acknowledge that “there is one relationship that circumvents this constraint, *namely the optical theorem*, (based on probability conservation) in which a rate bilinear in amplitudes is related to a rate linear in intensities, although only in a special way (namely, utilization of the real part of the forward reaction amplitude).”

Arash et al., also mention a proposal of Stodolsky[35] who had earlier pointed out the same “loop-hole” by suggesting an “interesting time reversal test with polarized targets” by measuring slow neutron-nuclei forward scattering.

Quoting Stodolsky almost verbatim, for spin vectors of neutron and target respectively, he “imagines (beam polarizations) \mathbf{s}_n and \mathbf{s}_T to be at right angles to each other, and to the *beam direction* \mathbf{m} . Then, to restore the original direction, he performs a 180° around, say, the \mathbf{s}_n axis, which reverses the direction of \mathbf{s}_T . Thus time-reversal invariance requires

$$F_{\mathbf{s}_n, \mathbf{s}_T} = F_{\mathbf{s}_n, -\mathbf{s}_T} \quad (11)$$

¹⁰ The discussion will continue to be ambivalent as to the separate identification of T- and P-violation. Since charge conjugation plays no obvious role in p, p scattering, it is hard to avoid invoking PCT conservation, which would imply that any T-violation has to be canceled by a P- violation.

where x and y are meant to show that \mathbf{s}_n and \mathbf{s}_T are oriented perpendicular to each other, and to the beam axis z . In other words, detection of time-reversal violation favors regions centered where

$$F \sim (\mathbf{s}_n \times \mathbf{s}_T) \cdot \mathbf{m} \quad . \quad (12)$$

is maximal¹¹

Stodolsky continues by suggesting theoretically plausible sources of such a term in the forward scattering amplitude. Though useful for a neutral particle such as the neutron, for charged particles, Rutherford scattering, peaking forward and back, makes the forward nuclear scattering amplitude immeasurable for charged particles. One cannot, therefore, consider using the optical theorem for p, p scattering.

5. Detection chamber polarimeter properties

Referring back to the Arash et al. categorization into experiment types, this proposed experimental configuration might seem to fit into the type (ii) “self-conjugate” type—forward-time and reversed-time reactions being measured with identical apparatus. This is not precisely the case, however. The beam currents of bunch 1 and bunch 2 will not be exactly equal, and their spin directions reverse under time reversal. Neither will the apparatus be exactly left-right nor exactly up-down mirror symmetric.

Formally, the experimental apparatus is of category (i)—it is not exactly self-conjugate. But the apparatus is very nearly symmetric in most ways and there are beam-based procedures that can greatly reduce normalization systematic uncertainties to well below levels values that Arash et al. suggest may be irreducible. Furthermore, with nearly full solid angle aperture coverage, rate determinations become branching ratio determinations rather than cross section measurements.

Whereas the “denominator” in a small aperture cross section measurement is a hard-to-determine solid angle, our branching ratio normalizing factor is a fixed total number of “good” events. Small solid angle apertures and near 4π solid angle denominators are both subject to systematic error, but the fractional error is much less for solid angles approaching 4π . Furthermore, expressed as a branching ratio, the same denominator will be common to the two rates being compared. Though the experiment is of category (i) in the Arash labeling, the normalization uncertainty can become small relative to counting statistic errors.

The tracking chamber plate thicknesses must be thin enough that no particles “range out undetected” even at the lowest particle energy. Best foil thickness compromises have been worked out, especially, by Ieira et al.[36]. (A very small set of) their measured analyzing powers for scattered proton polarimetry are shown in Fig. 10.

As predicted by Plottner and Bacher[37], under not unlikely conditions elastic scattering analyzing powers are guaranteed to be exactly 1 at some energy and direction in phase space.

Their conclusion is based on the understanding, for the scattering of initially unpolarized spin- $\frac{1}{2}$ particles from particles without spin, that the polarization P of the scattered beam can be expressed in terms of two complex quantities f and g , the non-spin-flip and spin-flip components of the scattering amplitude, functions of the scattering angle θ and of the energy E , as

$$P = \frac{2\Im(fg)}{f^2 + g^2}, \quad (13)$$

where the amplitudes f and g , can in turn be expressed in terms of partial wave phase shifts.

Measurements of Przewoski et al.[38] confirmed this for proton carbon-12 elastic scattering in the laboratory energy and angular ranges $160 < T < 200$ Mev and $12^\circ < \theta_{\text{lab}}^\circ$. In terms of $\Delta T = T - 183.1$ MeV and $\Delta\theta = \theta - 17.75$ degrees, their measurements were well fit by the formula

$$A(\theta, \Delta T) = 1 - \alpha\Delta T^2 - \beta\Delta T\Delta\theta - \gamma\Delta\theta^2, \quad (14)$$

with coefficients

$$\begin{aligned} \alpha &= 1.21 \pm 0.07, \\ \beta &= 1.61 \pm 0.11, \\ \gamma &= 1.00 \pm 0.07, \end{aligned} \quad (15)$$

in matching units.

These results are applicable to carbon-12 in any form. Graphite may be impractical as plate material for a tracking chamber; perhaps industrial multiplane graphene could be used. Graphite foil, such as used by Ieira[36] at much lower proton energies is probably inappropriate. The graphite plates might have to be sandwiched between thin conducting foil, such as aluminum which, itself, provides significant polarization analyzing power. The polarimetric properties of low- Z materials do not depend strongly on Z [39].

From existing measurements and models, with both initial spin states being known with near certainty, the left/right and up/down asymmetries of every scattered proton can be predicted with quite good accuracy. Based on the one million primary scatters for which at least one p -carbon scatter is observed, the dominant statistical uncertainty in dual-detected scatters will come from fluctuations in the p -carbon scatter of the other proton.

¹¹ Since the condition expressed in Eq. (12) was derived assuming collinear incident beams, its application in the current situation is murky, other than suggesting that, for sensitivity to symmetry violation, nether spin direction should be parallel to either incident beam direction.

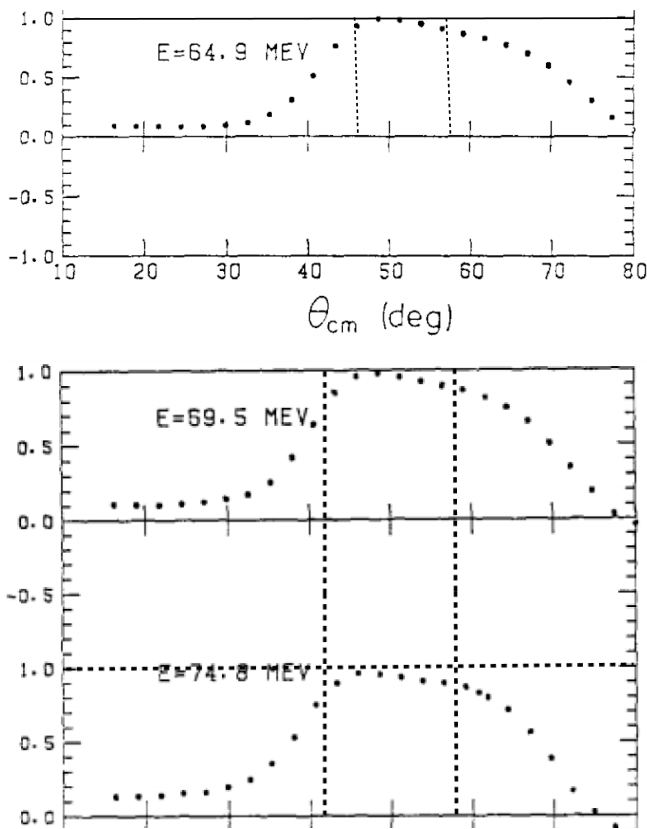


FIG. 10. Center of mass energy analyzing powers for left/right carbon-scattering proton polarimetry[36]. At all energies shown the analyzing power peaks above 0.99 and remains higher than 0.9 in the angular range from (for example) 45 to 60 degrees, where it can be accurately approximated by a polynomial fit tangent to the point at which the efficiency is 100 percent. With angular bins of one percent width in analyzing power, regions of predictably-high probability spin-flip violation can be accurately delineated. Extended from 100° to 170° , the plots are mirror symmetric about $\pi/2$. Since the angular distribution is known to be quite accurately isotropic, this high sensitivity region represents roughly 1/4 of all events. Of these an elastic scatter occurs with high probability in the first 1/4 of the proton stopping range. Especially valuable will be the one in 400 fraction of single scatters for which the polarizations of both scattered particle are measured with high analyzing power.

VII. UNBALANCED SPIN-FLIP T-VIOLATION DETECTION

1. The lore concerning elastic p, p scattering

A definitive early review of low energy p, p scattering was written in 1950, by J.D. Jackson and J.M. Blatt[40], (here J&B). Copying verbatim, their second paragraph reads

“The theoretical interpretation of proton-proton scattering experiments has been given in the classic papers of Breit and collaborators’ which not only constitute the pioneer work in this field, but also contain an exhaus-

sive treatment of the subject. For both neutron-proton and proton-proton scattering at low energies (below 4 Mev) the de Broglie wave-length of the nuclear motion is large compared to the range of nuclear forces. Hence the nuclear interaction is effective only in the S-states (zero-orbital angular momentum) of the two-particle system. (Experimentally, attributed almost entirely to S-wave scattering up to appreciably higher energies, of the order of 10 Mev.) The exclusion principle limits the possible states of the proton-proton system. Two protons in an S-state, in particular, have to have anti-parallel spins (be in the singlet spin state). The triplet spin state is forbidden. The S-wave proton-proton scattering thus involves only one nuclear phase shift, the one for the 1S -state. In contrast to this, neutron-proton S-wave scattering involves two phase shifts, for the 1S -state and 3S -states respectively.”

J&B are implicitly applying a general “exclusion principle” here, to limit the possible states of the p, p system. Without this, since the initial proton states are created incoherently, clearly the triplet spin state is *not* forbidden. Because the protons in both input and output states are indistinguishable, and (in the CM system) the protons are collinear, there can be no way to experimentally associate a particular input state proton with a particular output state proton. Though J&B apply this principle only at a very low 4 MeV energy, the same principle is presumably applicable at all energies. However, the strict limitation implied for possible spin states is specific to the low 4 MeV energy. *The application of this indistinguishability principle in Derbenev geometry is disputed in the present paper.* Observed in the laboratory, for the vast majority of all collisions, there is no difficulty in associating unambiguously each scattered proton with a particular incident beam.

Fifteen years later, in 1965, in the third edition of their book, Mott and Massey[15] repeat the same Jackson-Blatt argument concerning possible spin states and add as well: “Analysis of the earliest observations which provided definite evidence of the nuclear scattering of protons in hydrogen showed that the non-Coulomb interaction between two protons cannot be very different from that between a neutron and a proton in in an S^1 -state.” It had been confirmed by then that, in fact, the non-electrical forces between nucleons are independent of the nucleonic charges—the so-called charge independence of nuclear forces. Proposed initially by Heisenberg[41] before 1941, *this isotopic spin conservation principle, has been confirmed by overwhelming evidence ever since, and is accepted without dispute in the present paper.*

2. Coarse integrated polarimetry averaging

There is a clear statistical advantage for triplet incident states in which particle spins in both beams are all “up” or all “down”. In this case, there could be an overwhelming preservation of the same overload in the

scattered states. This would improve the selectivity for detecting scatters with unmatched spin flips.

But these are states for which T-violation is unlikely. Previous discussion has suggested that T-violation (or P-violation) detectability favors spin configurations for which triple products formed from the spin vectors of incident or scattered particles, along with any momentum vector, do not vanish. For long spin coherence time (SCT) one favors incident conditions with predominant “up” (or “down”) polarization for both incident bunches. To maximize T-violation sensitivity this vertical component is best augmented by mutually orthogonal transverse polarization components.

It is experimentally challenging to maintain beam polarization at fixed polar angle relative to “up” or “down”. However, this requirement is similar to optimal conditions for EDM measurement, for which the spin remains horizontal, always pointing approximately forward or backward, with polar angle equal to $\pi/2$). Such beam polarization stability has been successfully achieved in COSY.[10].

The “analyzing power” A in left/right scattering asymmetry for N scattered particles is defined by

$$A = \frac{R - L}{R + L} = \frac{R - L}{N}, \quad (16)$$

where R , L , and $N = R + L$ are, respectively, the numbers of right, left, and total scatters. Though R and L are stochastic quantities, subject to counting statistic uncertainty, it is usually legitimate to treat N as the unambiguous total number of scatters. In this case it is a branching ratio, rather than an absolute cross section, that is being determined. It is then natural to introduce normalized “branching ratios” satisfying the relations

$$p = n_R = R/N; \quad q = n_L = L/N; \quad p + q = 1, \quad (17)$$

where p is the right-scatter probability and q is the left-scatter probability. Substitution of these equations into Eq. (16) produces

$$p = \frac{1 + A}{2}; \quad q = \frac{1 - A}{2}. \quad (18)$$

On the other hand, the “efficiency”, E , in scattering asymmetry covers the common situation in which R and L are normalized by a number N_{incident} which is the total number of particles passing through the polarimeter, most of which register neither in the right nor the left detector. Then one defines efficiency E as the fraction of incident particles that actually register in the polarimeter;

$$E = \frac{N}{N_{\text{incident}}}. \quad (19)$$

In this case it is appropriate to treat N as stochastic.

Usually, in polarization measurement, there has to be a trade-off made between high efficiency, mediocre analyzing power, and low efficiency, high analyzing power.

What has typically been used in historic p, p polarization measurements can be characterized as low efficiency, $E < 0.0001$, and fair analyzing power, $A_{\text{min}} \approx 0.4$.

Along with the high efficiency $E \approx 1/400$ (the probability that an 183 MeV proton stopping in carbon will suffer an elastic nuclear scatter) the main design concept for the present proposal is to concentrate on detection of scatters for which polarimeter analyzing powers are as close as possible to 100%. In any case, best T-violation selectivity will require strong weighting of data from high analyzing power regions.

Selective detection of T-violating scatters depends critically on the analyzing power of the polarimetry, which is, itself, dependent on scattered proton energy. For best selectivity it is appropriate to weight most heavily data in regions for which the analyzing power is highest.

3. Figure-eight luminosity penalty estimate

4. Anticipated data rates

Anticipated data rate performance can start with the calculated storage ring luminosity of 10 inverse millibarns per second, capable of producing $N_0 = 2 \times 10^9$ clean scatters per year. Of these events, a number $N_1 = 10^7$ will provide p -carbon polarimetry for one or other of the final state protons, including $N_2 = 25,000$ for which both final state proton spins have been measured; with a fairly small fraction of these referred to as “gold-plated”, these events are “silver-plated”. All these rates are tabulated in Table I.

Note, however, that in a certain sense, modulo polarimetric inefficiency, the kinematics, including spin, of every one of the $N_1 = 10^7$ single polarimetric-detected events have been fully-determined. This assumes time-reversal symmetry, along with the concession that time-reversal violation will occur only at the one percent level. One hopes this fraction will exceed one percent but cannot expect this to reduce the sample size appreciably. From these data rates it is not obvious which class of events holds the best statistical power for detecting T-violation.

event class	symbol	formula	fraction	symbol	events/year
p, p scatter	N_0	1	1	N	2×10^9
single spin meas.	N_1	$2/E$	$2/400$	N_1	1×10^7
double spin meas.	N_2	$2/E^2$	$2/400^2$	N_2	0.25×10^5

TABLE I. Anticipated event rates with increasing detection quality per nominal year running time for polarimetric detection efficiency $E = 1/400$.

Let us consider the experimental problem of detecting a correlation between initial and final spin coordinates, on the one hand, and scattering directions on the other. Based on many historic experiments, experimentally measured cross sections have been parameterized to

best fit, PCTC (P and T-conserving) theoretical production models. These distributions have been and can now be digitally reproduced with high accuracy by Monte-Carlo simulation, as parameterized by best fit partial wave expansion coefficients.

One now speculates that, hidden in this data, is a PCTV, time-reversal violating contribution with differential cross section at perhaps the one percent level, which has so far evaded detection. We propose, therefore, to study the same process by direct measurement. This might be called “analog Monte-Carlo determination”. The reason we have to acknowledge the stochastic nature of the measurement, is that we have only beams with less than 100% polarization and polarimetry with less than 100 percent analyzing power.

A requirement of T-symmetry is that, if one spin flips, so also does the other. The PCTC (P-conserving, T-conserving) fit presumably satisfies a constraint $N_u = N_{\text{null}}$ where N_{null} is the (dominant) theoretical rate, calculated from already-known “measured cross sections” with no apparatus equipment prejudice concerning the fractional contribution of T-violating or P-violating processes, but the theoretical expectation that these contributions have been smaller than some small value, such as one percent.

In our proposed experiment, frozen-spin monochromatic protons in independently adjustable (almost) pure spin states collide inside a nearly 4π acceptance polarimeter. The CM system motion in the lab is modest and scattered energies are identical. Both scattered particles will stop in nearly full-acceptance tracking chambers. Some will undergo nuclear scatters in the tracking chamber plates. This will provides polarimetry, for example with efficiency $E \approx 1/400$ and analyzing power $A \approx 0.96$.

At the cost of some duplication, to reduce confusion between scattering statistics and polarimetry statistics, one can switch variables in formulas (16) through (19) from R and L to N_u and N_d , which are the (unknown) numbers of “up” and “down” protons in a scattered beam. In the proposed experiment this amounts to treating p, p scattering as “virtual polarimetry” for which the “up” or “down” state of each scattered proton has not yet been detected.

For convenient reference to conventional statistics notation we will, however, retain p and q , satisfying $p + q = 1$, as the probabilities of events satisfying the binomial distribution. And, for numerical example in the proposed experiment, the typical numerical values of analyzing power and efficiency are very different from conventional polarimetry.

For example, we use the value $A = 0.96$, which produces $p = n_u = N_u/N = 0.98$ and $q = n_d = N_d/N = 0.02$ with p and q fractional (i.e. summing to 1) binomial distribution probabilities. As a binomial distribution, standard deviation about the mean (the same for both N_u and N_d) is given by

$$\sigma_{\text{binomial}} = \sqrt{Npq} \stackrel{e.g.}{=} 0.14 N^{1/2}. \quad (20)$$

Quoted with error bars, relative to the null-expected rate, according to this standard deviation, the measured up-rate will be

$$N_u = pN_{\text{null}} \left(1 \pm \sqrt{\frac{pq}{N}} \right) \stackrel{e.g.}{=} \mathbf{N_{u,measured}} \left(1 \pm \frac{0.14}{N^{1/2}} \right), \quad (21)$$

where (with $\mathbf{N_{u,measured}}$ shown bold-face for emphasis) the statistical significance of deviation from a null distribution mean can be quantified by its magnitude in units of the “ \pm error” term. The merit of this formulation in the present context is that the error can be calculated without the need for having actual data.

For the sake of definiteness, let us tentatively presume a current upper limit T-violating contribution of $\hat{\sigma}^{\text{current T-ViolFrac}} = 0.01$ exists, with error bars $\pm\sigma_{\text{meas.}} = \pm 0.01$. This would match the supposition that any higher fraction would have already been detected. The experimental challenge will be to produce a T-violation signal with systematic error smaller than the counting statistics error. We substitute $N = 5 \times 10^6$ into Eq. (21) to produce an estimated fractional statistical error

$$\sigma_{\text{est.}} = \frac{0.14}{2236} = 0.63 \times 10^{-4}, \text{ or} \\ \text{T-ViolFrac} = 0.01 \pm 0.63 \times 10^{-4}. \quad (22)$$

Preliminary and vague as it is, this evaluation is given only to suggest that T-violation at significantly low levels should be achievable.

Averaged over all directions, this fractional error is likely to be misleading since the measured polarizations themselves may tend to cancel on average. More granular estimations, based on judicious preparation of the incident bunch polarizations, follow.

5. Two particle T-violation detection

The binomial distribution, for N_2 trials, of “success” with probability p and “failure” with probability q is

$$P(x) = \frac{N_2!}{(N_2 - x)!x!} p^x q^{N_2 - x}. \quad (23)$$

It is instructive for understanding the logic, to start by calculating the probability of correct determination for a single particle spin flip using a polarimeter with mediocre probabilities, such as $p = 0.58$, $q = 0.42$. Already with 10 events, the average success probability exceeds 1/2. For data sets with N_2 increasing arbitrarily beyond 10, the success probability approaches $p = 0.58$ and the failure probability approaches $q = 0.42$.

Supposing (with no justification) that protons from a 100% “up”-polarized beam produce only “up”-polarized scatters, consider a scattered proton entering a polarimeter for which $p = 0.58$ represents the probability of its spin state being properly identified. Further supposing

T-violation consisted only of events with one spin flipping and one not, p and q could be described as “null probabilities” in the sense that, with no T-violation, the true distribution has no spin flips. In the large sample limit a collected data set would then be expected to center on $x = 0.58$, because this is the fraction of correctly identified polarizations.

Contemplating the presence of some T-violating scatters, we would interpret deviation of the peak position from $x=0.58$ as indication of T-violation. Regrettably, we do not actually “understand the probabilities”. The true analyzing power will not, in fact, be constant, independent of kinematic parameters, nor will it even be exactly equal to $A = 0.4$ “on the average”. Though ameliorated by calibration efforts, this will inevitably leave detection of T-violation, purely on the basis of deviation from a calculated value (such as 0.58) as unreliable.

In conventional language, for small samples, the uncertainty will be dominated by statistical uncertainty but, for large samples, the uncertainty will be dominated by systematic errors resulting from our imperfect understanding of the apparatus.

To reduce this systematic error it is important for the polarimeter analyzing power to be as high as possible— at 100% there would be no systematic error. In the proposed experiment, only a tiny fraction of the detected scatters will have analyzing power greater than 0.99, but a substantial fraction will have a, still respectable, analyzing power greater than 0.9.

In an experiment intending to investigate time reversal conservation the distinguishing signal for T-violation is that, if one spin flips, so also must the other. If spin-flips were forbidden by T-conservation (*which they are not*) then any detected spin-flip would provide evidence for T-violation. To reduce confusion it is sensible for initial spin states to be set up to be all the same, say “up”. Then any detected “down” polarized scattered proton would provide evidence of T-violation. Since *some T-conserving amplitudes do involve spin-flips*, the true situation would be much more complicated, except for the fact that, for T-conservation in elastic scattering if one spin flips, so must the other. T-conserving scatters must “match” in this sense.

As a consequence, except for different interpretations and values for the p and q probabilities, the T-violation probabilities associated with correctly identifying T-violation using “mismatched” spin flips is described by the same binomial distribution, Eq. (23), as for the single particle T-violation described previously.

The least ambiguous signature for T-violation is one spin flipping, and the other not. Actually, both identifications being wrong provides information equivalent to both being correct, as far as T-violation detection is concerned. As a result, in a 98% analyzing power set-up, the two particle correct T-violation identification probability is: $0.98 \times 0.98 + 0.02 \times 0.02 = 0.9608$. The probability of one correct and one incorrect identification is $2 \times 0.02 \times 0.98 = 0.0392$. Conservation of probability,

confirmed by summing the probabilities, is reassuring.

Let us assume $N_1 = 5 \times 10^6$ events, for which all kinematic parameters are known and at least one scattered particle’s polarization, have been recorded. For each event there is also a recorded “phase angle” ψ providing the instantaneous orientations of both input spin vectors in spin-space. For now this is just a tallying mechanism for associating the instantaneous polarization measurement with the other particle parameters in effect when the polarization measurement was made. Each of the measured polarization values can then be compared with the previously established “null polarization values”.

Of the events just discussed, about $N_2 \approx 0.25 \times 10^5$ events, will contain spin information about both scattered particles. Some, with almost 100 percent analyzing power, were referred to earlier as “gold-plated”. Even a few events in which one spin flipped, and one did not, would prove the existence of T-violation. Further statistical analysis of these events is far too difficult to be attempted in the present paper.

VIII. APPLICATION OF “SPIN TRANSPARENCY”

1. History

The concept of “spin transparency”, was introduced and defined in 2016 by Derbenev[8]: “In a figure-8 collider, the spin first rotates about the vertical field in one arc. This rotation is then undone by the opposite field in the other arc. The resulting effect of the “strong” arc dipoles on the spin dynamics reduces to zero over one particle turn and the whole ring becomes “transparent” for the spin.” The concept is more fully developed and explained in Filatov et al. [11] In the context of the present paper, it is spin transparency (which is unrelated to “spin filtering”) that contributes to nuclear spin physics by providing the accelerator physics capability to study T-violation in low energy nuclear physics.

A property that makes the term “transparency” apt, is that, regarded as an approximate method, the transparency approximation can usually be most valid for slow changes on long (adiabatic approximation) time scales. The next section shows how adiabatic sinusoidal variation of beam spin states can provide Fourier sensitivity enhancement to enable experimental detection of T-violation in p, p scattering.

2. Adiabatic Fourier sensitivity enhancement

”Can One Hear the Shape of a Drum?” is the title of a 1966 article by Mark Kac in the American Mathematical Monthly which made this question famous. Not having read the article (since the title expresses a question rather than an answer) one can ask a similar question in the present context: “With the proton assumed to

be composite, rather than elementary, can internal proton variability have a measurable effect on “elastic” p, p scattering?”.

A routine procedure of experimental mechanical engineering is to scan in frequency a harmlessly small sinusoidal signal applied judiciously to a physical structure, in order to determine frequencies at which strong drive might be harmful. Applying the principle that any linear response must have the same frequency as the drive, synchronous detection can enhance the sensitivity by a large factor.

Here, for elastic proton scattering, we conjecture that the answer to the rhetorical question above is “yes”. A collision between two protons could temporarily stir up the contents of the protons enough to affect the elastic angular scattering distribution while producing no other detectable particles nor any measurably-large reduction of proton energy.

A phase angle ψ is introduced in Fig. 11 with the considerations just introduced in mind. A way suggested to enhance the statistical sensitivity to T-violation is to vary ψ sinusoidally and detect the polarimetric response synchronously.

Fourier series capability is especially valuable for statistically “noisy” data. In our case the statistical power of individual events varies over such a large range that most of the events provide little help in studying spin dependence. A bias-free strategy for filtering promising events from useless events is needed. With relatively few significant Fourier coefficients being expected, for example three, constant term plus fundamental harmonics, it is useful to allow every event to contribute to every coefficient, with the expectation that the contributions from especially noisy events will average to zero.

This Fourier series capability should be especially useful for analyzing the $N_1 = 5 \times 10^6$ “silver-plated” events for which the spin of just one final state proton has been measured. The data sets will be periodic functions of the ψ -phase angles. With the data represented as a periodic function, with period 2π , it is natural to convert the data sets into Fourier series. The proton beam polarization could advance nominally (for example) as $\mathbf{s}_p = \cos \psi \hat{\mathbf{x}} + \sin \psi \hat{\mathbf{y}}$, but with individual bunch phases separately adjusted. The T-violation evidence will then be contained primarily in the constant term plus the lowest harmonic sine and cosine coefficients of the Fourier series expansions of the data sets.

The uncertainties in these T-violation determinations should then be dominated by statistical errors. The systematic error should be quite small, since the data will be “self-normalizing”; the normalization will be established by the constant term of the Fourier series. Presuming that the double-polarization data is more statistically significant, the single particle measured polarization data, should provide a self-consistency check.

One can also consider restricting the analysis to regions for which the polarimetry analyzing power is well above average. A significant fraction of p, p scatters will have

laboratory scattering angles corresponding to the central CM angular ranges shown bounded by broken lines in Fig. 10. In this range the polarimetry analyzing power starts above 97%. Furthermore, mentally-interpolating from the upper and lower plots in Fig. 10, the analyzing power will exceed, for example, 70%, for a substantial fraction of their full-ranges in the tracking chamber.

IX. RECAPITULATION AND ACKNOWLEDGMENTS

The thesis of the present paper is that p, p scattering near the pion production threshold represents the most promising region for the investigation of wave particle duality, by experiment and theory.

The regions of validity of “correct” theories in physics are always bounded. Certainly the region under discussion represents a boundary beyond which classical mechanics ceases to be valid. Alternatively, this region represents a boundary below which quantum physics becomes unnecessary. Here the word “quantum” is ambiguous. As introduced by Planck, the term quantum applied to massless “particles”. As applied in elementary particle physics, the term has come to apply also to massive unstable particles.

Without a doubt, the Einstein formula $\mathcal{E} = mc^2$ corrects Newtonian mechanics for massive particle speeds that are not negligibly small compared to the speed of light. But, when the “mass” of an unstable particle comes into question, so also does the Einstein formula. To good approximation, this issue is addressed by the Heisenberg time uncertainty principle; but this may represent only a temporary “fix” for the Einstein formula and quantum mechanics. The p, p region under discussion is most appropriate for investigating this issue experimentally.

The issue of angular momentum is more serious. There seems to be some kind of trade-off, among mass, spin, and angular momentum. Surely, quantum mechanics, as augmented by the incorporation of spin 1/2 by Pauli and Dirac, provides an unquestionably valid and accurate theory of atomic physics. But the p, p scattering region under discussion calls these ideas into question for nuclear physics. And “Why does the muon ‘weigh?’” continues to demand some kind of answer.

The “center of mass” concept is central to quantum mechanics, but foreign to special relativity, where it is a mathematical abstraction, of no instantaneous geometric significance. The upper and lower pairs of Dirac spinor amplitudes could just as well represent fractional negative and positive mass fractions in a classical sense. The muon (like the electron, but unstable) could play the transitory role of smoothing over the kinks and distortions in the transmutation from two p, p to three p, p, π “particles” with the π itself unstable, and the neutrino invisibly cleaning up the resulting mess.

This could very well cause the outcomes in parallel in-

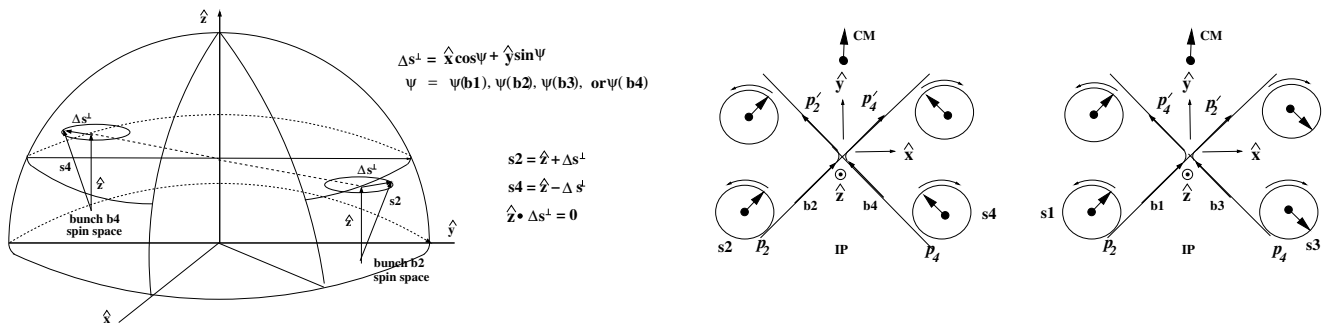


FIG. 11. Exploiting adiabatic spin transparency, beam spin orientations can be scanned coherently, for example to achieve Fourier series statistical enhancement of T-violation detection sensitivity; see Section VIII 2. **Left:** Two of four beam bunch spins are shown. Colliding pairs are **b1,b3** and **b2,b4**. Phase angles ψ are externally controllable independently for each of the four beam bunches. **Right:** Spins of bunches **b1** and **b2** are the same, **b3** and **b4** opposite. Preparation of two or more deuteron bunches in individualized spin states as assumed in this figure, could be demonstrated immediately at COSY, using the methods described in reference [28].

cidence and perpendicular incidence to be strikingly different. The proposed apparatus could demonstrate such differences, In glancing collisions in DERBENEV geometry, the geometric distortions in glancing collisions can be more easily visualized than in WOLFENSTEIN geometry.

This paper has shown, in Sections III through III 6, that correct relativistic treatment of the “anomalous” magnetic moment of the proton explicitly contradicts p, p time reversal invariance by the unavoidable introduction of spin precession in (weak, but unavoidable) magnetic field encountered during scattering through a finite angle. It also suggests, for example in Figure 9, a treatment of scattering from spheres resembling that of Van de Hulst[18]. The near coincidence between deBroglie wavelength and proton radius, shown in Figure 8, and pion threshold, shown in Figure 6, can hardly be accidental.

Almost a century after the beginning of nuclear physics (in Europe, mainly German-speaking, by Heisenberg, Wigner, Fermi, Bethe, Chadwick, and others) p, p scattering is described entirely by phenomenological partial wave analysis, which makes very little sense either experimentally or from any fundamental theoretical perspective. The footnote below, copied verbatim from page 415 of Stratton’s book[43],¹² anticipated the problem.

Neither the book by Van de Hulst[18] nor by Stratton ever mention the term “angular momentum” nor partial wave expansion, while, at the same time, describing a formalism more nearly matching observable characteristics

of p, p scattering.

The history of modern physics can be encapsulated in a few sentences (cut and pasted from the web): Johannes Kepler enunciated his laws of planetary motion in 1618. Galileo officially faced the Roman Inquisition in April of 1633 and agreed to plead guilty in exchange for a lighter sentence. Newton unified Galileo’s theory of falling bodies with Kepler’s laws of planetary motion. He published his laws of motion and universal gravitation in 1687. Albert Einstein’s 1905 theory of special relativity is one of the most important papers ever published in the field of physics. Bill number 246, debated by the Indiana General Assembly in 1897, proposed establishing by law the value of π to be 3.2. The bill never became law due to the intervention of Prof. C. A. Waldo of Purdue University. And so on, as described above in this paper.

In its wisdom, and not to be outdone by the state of Indiana, the German government has determined that COSY has outlived its usefulness. This paper has attempted to make the case that this action rivals the Roman Inquisition in stupidity. The correct description of power generation by nuclear fusion relies on the correct understanding of nuclear transmutation, which can only proceed from a correct understanding of nucleon, nucleon scattering. Certainly the cost of the program proposed in this paper is negligible in comparison to the cost and necessity of the development of power generation by nuclear fusion.

I wish to acknowledge the valuable hints, corrections, or enthusiasm, by Kurt Aulenbacher, Yunhai Cai, Slava Derbenev, Eanna Flanagan, Susan Gardner, Joe Grames, Kolya Nikoliev, Maxim Perelstein, Frank Rathmann, James Ritter, Joken Stein, Saul Teukolsky, to my son John and other COSY collaborators, and to discussions concerning the frontier between mathematics and physics during regular weekly meetings with Leonard Gross.

¹² The first thorough investigations of the electromagnetic problem of the sphere were made by Mie, *Ann. Physik.*, **25**, 377,1908, and Debye, *Ann. Physik.*, **30**, 57, 1909. Both writers made use of a pair of potential functions leading directly to our vectors **M** and **N**. The connection between these solutions and a radial Hertzian vector has been pointed out by Sommerfeld in Riemann-Weber, *Differentialgleichungen der Physik*, p. 407, 1927.

Appendix A: Consistent treatment of g, G and $g \rightarrow G$

1. Orders of magnitude

A chronological listing for the values of nuclear physical constants includes, for example, (2014 values), (2010 values) (2006 values) (2002 values) (1998 values) (1986 values) (1973 values) (1969 values)[16] For example, “Atomic Weights and Isotopic Compositions for All Elements”.[17]

The following statements, all expressed in MKS units, can be made about protons, electrons, and protons, as they enter this paper:

1. The radius of the proton is about 1 fm (10^{-15} m), smaller than the radius of a hydrogen atom by a factor of 60,000.
2. The “classical radius” of a particle is given by $r^{\text{class.}} = e^2/(4\pi\epsilon_0 mc^2)$, where e and m are the charge and mass of the particle. This is the radius a charge having mass m would have if its mass (uniformly distributed) and energy (derived according the E&M) were related by the Einstein formula.
3. The classical radius of the electron is given by $r_e^{\text{class.}} = 2.8179403262 \times 10^{-15}$ m, roughly three times the measured proton radius $r_p^{\text{meas.}} \approx 1$ F (for Fermi), but immeasurably greater than the electrons actual radius, since the electron is considered to be and treated to be “point-like”. (Mnemonic: if the (spherical) proton’s interior had its own charge and an electron’s charge superimposed continuously and uniformly, the overall system would be uncharged”.)
4. The de-Broglie wavelength of a non-relativistic particle of mass m and kinetic energy K satisfies the equations $\lambda = h/p$, $K = p^2/(2m)$, $p = \sqrt{2mK}$. Applied to electrons and protons;

$$\lambda_e^{\text{de-B}} \approx h/\sqrt{2m_e K_e}, \quad \lambda_p^{\text{de-B}} \approx h/\sqrt{2m_p K_p}.$$

$$\frac{\lambda_e^{\text{de-B}}}{\lambda_p^{\text{de-B}}} = \sqrt{\frac{m_e}{m_p} \frac{K_e}{K_p}}$$

which, for comparison of electron and proton inelastic scattering is approximately

$$\sqrt{\frac{1}{2000} \frac{20 \text{ eV}}{100 \text{ MeV}}} \approx 10^{-5}$$

5. For an electron with $KE = 1$ eV and rest mass energy 0.511 MeV, the associated DeBroglie wavelength is 1.23 nm, about a thousand times smaller

than the wavelength of a 1 eV photon; a 1 eV photon has a wavelength of 1240 nm, with negligible uncertainty.

6. The Compton wavelength of a particle is given by $\lambda^{\text{Compton}} = hmc$. The Compton wavelength of the electron is $2.42631023867(73)10^{-12}$ m, 2000 times smaller than the proton Compton wavelength, which is therefore about 10^{-9} m.
7. The kinetic energy threshold for pion production in proton-proton collisions is 280 MeV,
8. These numerical examples serve as reminders or the huge differences in orders of magnitude of potentially relevant physical parameters. The near coincidence between deBroglie wavelength and proton radius, shown in Figure 8, and pion threshold, shown in Figure 6, can hardly be accidental.

2. Integer arithmetic, $g \rightarrow G$

The data table below exhibits $g \rightarrow G$ conversion using of integer arithmetic—this issue applies only to values of m in the “Atomic mass” column, from NIST tables[16][17]; integer entries have no decimal points and integer arithmetic is used in the evaluation of $G = (g \times m/Z - 2)/2$. The motivation for this is that, along with the obvious requirement that the values of m have to be identical in the evaluation of g and G , there are no transcendental numbers in the relation between g and G . The importance of respecting this discipline is apparent in many examples in the table; powers of ten, indicated by exponential notation appearing in m column, show up as corresponding trailing zero digits in G denominators.

The first task is to best approximate g as a ratio of integers $g \approx n/d$, with denominator $d < 100$, plus a correction provided by the most accurate value of m available. The maximum value 100, was chosen such that at least the first four digits of the g correction were zero—meaning accuracy, roughly speaking, to better than one part in ten thousand..

Because the deuteron to proton mass ratio is known to such high accuracy three determination are given; the surprising $g - G = 1$ at low accuracy is seen, at higher accuracy, to be simple coincidence. In most other cases two evaluations are given. In the cases of lithium, boron, and silver, two stable isotopes are treated. This provides warning that the purity of samples needs to be taken into account.

Other than noting that all entries have been taken from NIST tables, the sources of entries and their errors are not given in this paper; in fact most values of m simply been truncated to seven digits, to reduce confusing complexity. In every case the three lines providing “Relative Atomic Mass”, “Isotopic Composition”, and “Standard Atomic Weight” have been cut and pasted from NIST tables, [16][17]—simple detective work can then identify most of the sources. As far as I know there are no reliable tables providing accurate values of G .

%-----													
% first period													
Z	A	*/	element	S	g-fac(meas.)	ratio	correction	m	G=(g-fac/Z*m-2)/2				
%-----													
Z	A	*/	element	S	g-fac(meas.)	ratio	correction	Atomic-Mass	G-(rational)	G			
%-----													
1	1		H	hydrogen	0.5	+5.58569468	+391/70	-0.0000196	1000000/10 ⁶	251/140	+1.79285714	+147/82	+0.00017420
1	1		H	hydrogen	0.5	+5.58569468	+391/70	-0.0000196	1007825/10 ⁶	1451769/800000	+1.81471125	+49/27	-0.00010356
% Relative Atomic Mass = 1.00782503223													
% Isotopic Composition = 0.999885(70)													
% Standard Atomic Weight = [1.00784,1.00811]													
1	2		H	deuteron	1.0	+0.85743820	+6/7	+0.0002953	1998463/10 ⁶	-1004611/7000000	-0.14351585	-1/7	-0.00065870
1	2		H	deuteron	1.0	+0.85743820	+6/7	+0.0002953	2014101/10 ⁶	-957697/70/10 ⁶	-0.13681385	-13/95	-0.00002825
1	2		H	deuteron	1.0	+0.85743820	+6/7	+0.0002953	2014101778/10 ⁹	-478847333/35/10 ⁸	-0.13681352	-13/95	-0.0000282
% Relative Atomic Mass = 2.01410177812													
% Isotopic Composition = 0.000115													
% Standard Atomic Weight = [1.00784,1.00811]													
1	3	*	H	tritron	0.5	+5.95799369	+566/95	+0.0000989	2992631/10 ⁶	751914573/95000000	+7.91489024	+372/47	+0.00000337
1	3	*	H	tritron	0.5	+5.95799369	+566/95	+0.0000989	3016049/10 ⁶	566/95	+7.98465123	+519/65	+0.00003584
% Relative Atomic Mass = 3.0160492779													
% Isotopic Composition =													
% Standard Atomic Weight = [1.00784,1.00811]													
2	3		He	helion	0.5	-4.25499544	-217/51	-0.0000934	2992612/10 ⁶	-12549953/3000000	-4.18331767	-251/60	+0.00001566
2	3		He	helion	0.5	-4.25499544	-217/51	-0.0000934	3016029/10 ⁶	-286159431/68000000	-4.20822692	-101/24	+0.00010641
% Relative Atomic Mass = 3.0160293201													
% Isotopic Composition = 0.00000134													
% Standard Atomic Weight = 4.002602													
2	4		He	alpha	0.0	0.0			3971525/10 ⁶				
% Relative Atomic Mass = 4.00260325413													
% Isotopic Composition = 0.99999866													
% Standard Atomic Weight = 4.002602													
%-----													
% second period													
Z	A	*/	element	S	g-fac(meas.)	ratio	correction	m	G=(g-fac/Z*m-2)/2				
%-----													
Z	A	*/	element	S	g-fac(meas.)	ratio	correction	Atomic-Mass	G-(rational)	G			
%-----													
3	6		Li	lithium	1.0	+0.8220473	+60/73	+0.0001294	5968419/10 ⁶	-1331581/7300000	-0.18240836	-17/93	+0.000387330
3	6		Li	lithium	1.0	+0.8220473	+60/73	+0.0001294	6015122/10 ⁶	-642439/3650000	-0.17601068	-16/91	-0.000186504
% Relative Atomic Mass = 6.0151228874													
% Isotopic Composition = 0.0759(4)													
% Standard Atomic Weight = [6.938,6.997]													
3	7		Li	lithium	1.5	+2.170951	+165/76	-0.0001016	6961529/10 ⁶	+46176819/30400000	+1.51897431	+120/79	-0.00001303
3	7		Li	lithium	1.5	+2.170951	+165/76	-0.0001016	7016003/10 ⁶	+46776033/30400000	+1.53868529	+20/13	+0.00022375
% Relative Atomic Mass = 7.0160034366													
% Isotopic Composition = 0.9241(4)													
% Standard Atomic Weight = [6.938,6.997]													
4	9		Be	beryllium	1.5	-0.78495	-73/93	-0.0000037	8942209/10 ⁶	-1396781257/744000000	-1.87739416	-92/49	+0.00015686
4	9		Be	beryllium	1.5	-0.78495	-73/93	-0.0000037	9012183/10 ⁶	-467296453/248000000	-1.88425989	-179/95	-0.00004936
% Relative Atomic Mass = 9.012183065(82)													
% Isotopic Composition = 1													
% Standard Atomic Weight = 9.0121831													
5	10		B	boron	3.0	+0.600215	+3/5	+0.0002150	9935193/10 ⁶	-20194421/50000000	-0.40388842	-21/52	-0.00004226
5	10		B	boron	3.0	+0.600215	+3/5	+0.0002150	10012936/10 ⁶	-2495149/6250000	-0.39922384	-2/5	+0.00077616
% Relative Atomic Mass = 10.01293695													
% Isotopic Composition = 0.199(7)													
% Standard Atomic Weight = [10.806,10.821]													
5	11		B	boron	1.5	+1.7924326	+95/53	-0.0000202	10923826/10 ⁶	50776347/53000000	+0.95804428	+91/95	+0.000149543
5	11		B	boron	1.5	+1.7924326	+95/53	-0.0000202	11009305/10 ⁶	20635359/21200000	+0.97336599	+73/75	+0.000032656
% Relative Atomic Mass = 11.00930536													
% Isotopic Composition = 0.801(7)													
% Standard Atomic Weight = [10.806,10.821]													
6	12		C	carbon	0.0	0.0			11906828/10 ⁶				
% Relative Atomic Mass = 12.0000000													
% Isotopic Composition = 0.9893(8)													
% Standard Atomic Weight = [12.0096,12.0116]													
6	13		C	carbon	0.5	+1.4048236	+59/42	+0.0000616	12902393/10 ⁶	36748741/72000000	0.51039918	+49/96	-0.00001748
% Relative Atomic Mass = 13.00335483507													
% Isotopic Composition = 0.0107(8)													
% Standard Atomic Weight = [12.0096,12.0116]													
6	14	*	C	carbon	0.0	0.0			13894516/10 ⁶				
% Relative Atomic Mass = 14.0032419884													
% Isotopic Composition =													
% Standard Atomic Weight = [12.0096,12.0116]													
8	17		O	oxygen	2.5	-0.757516	-25/33	+0.000058	16867145/10 ⁶	-7597429/4224000	-1.79863376	-178/99	-0.00065396
% Relative Atomic Mass = 15.99491461957													
% Isotopic Composition = 0.99757(16)													
% Standard Atomic Weight = [15.99903,15.99977]													
9	19		F	fluorine	0.5	+5.257736	+510/97	+0.0000040	18850894/10 ⁶	131132599/29100000	4.50627488	+356/79	-0.0000542
% Relative Atomic Mass = 18.99840316273													
% Isotopic Composition = 1													
% Standard Atomic Weight = 18.998403163													
10	21		Ne	neon	1.5	-0.441198	-15/34	-0.0000215	19992440/10 ⁶	-4899433/3400000	-1.44100971	-134/93	-0.0001494
% Relative Atomic Mass = 19.9924401762													
% Isotopic Composition = 0.9048													

Standard Atomic Weight = 20.1797												

% fifth period, second row transition metals												
Z	A	*/	element	S	g-fac(meas.)	ratio	correction	m	G=(g-fac/Z*m-2)/2	G	ratio	correction

47	107		Ag silver	0.5	-0.22714	-5/22	+0.0001327	106905091/10 ⁶	-520505091/4136000	-1.25847459	-112/89	-0.0000476
% Relative Atomic Mass = 106.9050916												
% Isotopic Composition = 0.51839												
% Standard Atomic Weight = 107.8682												
47	109		Ag silver	0.5	-0.26112	-23/88	+0.0002436	108904755/10 ⁶	-2155361873/16544000	-1.30280577	-99/76	-0.0001742
% Relative Atomic Mass = 108.9047553												
% Isotopic Composition = 0.48161												
% Standard Atomic Weight = 107.8682												

Appendix B: Protons stopping in graphite

From Fig. 1 one sees, in right angle crossing collision geometry, that the laboratory frame is close to, but not quite equal to the center of mass (CM) frame. Nevertheless, in our orthogonal collision geometry, compared to laboratory fixed target scattering measurement, scattering symmetries are much better preserved. The horizontal, x, y , and vertical x, z planes are common to both laboratory and CM frames, thereby preserving left/right and up/down symmetries. Though elastically scattered protons are exactly collinear in the CM frame, they are more nearly orthogonal in our laboratory frame.

To simplify discussion, we will ignore the implied slow transverse velocity in the laboratory, taking it as the CM

frame. In this approximation, all CM scatters through $\pi/2$ lie in the same “orthogonal” plane, common to laboratory and CM frames and have azimuthal angles preserved, but polar angles are slightly distorted. Scattered particles have identical energies but not collinear paths.

Table II shows stopping powers and ranges for kinetic energies in the applicable range. With graphite density of 1.7 g/cm², all final state protons will stop in the graphite chamber, producing accurate energies for most scattered protons. Precision energy determination (for example to exclude inelastic scatters) depends on the full stopping range. But, since the p, C polarization analyzing power falls with decreasing proton energy, polarimetric analyzing power is provided mainly by the left/right asymmetry of p, C elastic scatters in the first half of their ranges, while their energies remain high.

- [1] R.M. Talman, *Superimposed Electric/Magnetic Dipole Moment Comparator Lattice Design*, ICFA Beam Dynamics Newsletter #82, Yunhai Cai, editor, 2021 JINST 16 P09006
- [2] R. Talman, *Difference of measured proton and He3 EDMs: a reduced systematics test of T-reversal invariance*, arXiv:2205.10526v2 [physics.acc-ph], <https://doi.org/10.1088/1748-0221/17/11/P11039>
- [3] T.D.Lee and L. Wolfenstein, *Analysis of CP-Invariant Interactions and the K_1^0 and K_2^0 system*, Phys. Rev. **138**, 68, 1965
- [4] J. Prentki and M. Veltman, *Possibility of CP violation in semi-strong interactions*, Phys.Letters15,88, 1965
- [5] L. B. Okun, *Remark on CP-parity*, Sov. J. Nucl. Phys., **1**, 1965
- [6] I.Yu. Kobzarev, L.B. Okun et al., *The Violation of CP Invariance*, <https://doi.org/10.1070/PU1967v009n04ABEH003013>
- [7] J. Gomez-Camacho, et al., *Time scales in nuclear structure and nuclear reactions of exotic nuclei*, Il Nuovo Cimento, 42, C, 2019
- [8] Y.S. Derbenev et al., *Siberian Snakes, Figure-8 and Spin Transparency Techniques for High Precision Experiments with Polarized Hadron Beams in Colliders*, Symmetry, 13, 398. <https://doi.org/10.3390/sym13030398>, 2021
- [9] A. Ashtekar, T. De Lorenzo, and N. Khera, *Compact binary coalescences: The subtle issue of angular momentum*, Phys. Rev D, 101, 044005 2020
- [10] CPEDM Group, *Storage ring to search for electric dipole moments of charged particles Feasibility study*, CERN Yellow Reports: Monographs, CERN-2021-003, 2021
- [11] Y. Filatov et al. *Transparent spin method for spin control of hadron beams in colliders*, Phys. Rev. Lett., 124, 194801, 2020
- [12] J. Blatt and V. Weisskopf, *Theoretical Nuclear Physics*, Dover Publications, 1991 reprint of Springer-Verlag, 1979, from John Wiley, 1952
- [13] G. Gamow and C. Critchfield, *Theory of Atomic Nucleus and Nuclear Energy Sources*, Scholar Select reprint of Oxford, at the Clarendon Press, 1949
- [14] C. Lechanoine-LeLuc and F. Lehar, *Nucleon-nucleon elastic scattering and total cross sections*, Rev. Mod. Phy, **65**, 1, 1993
- [15] N. Mott and H. Massey, *The Theory of Atomic Collisions*, Oxford, at the Clarendon Press, 1965
- [16] , *Background information related to the constants*, <https://physics.nist.gov/cuu/Constants/background.html>
- [17] , *Atomic Weights and Isotopic Compositions for All Elements*, https://physics.nist.gov/cgi-bin/Compositions/stand_alone.pl
- [18] , *Light Scattering by Small Particles*, Dover Publications, 1981 (originally, John Wiley and Sons, Inc. NY), 1957
- [19] S.D. Drell and A.C.Hearn, *Exact sum rule for nucleon magnetic moments*, Phys. Rev. **16**, 20, 1965
- [20] S.B. Gerasimov, Sov. J. Nucl. Phys. 2 430, 1966
- [21] K. Helbing, *Experimental verification of the GDH*

K.E.	Stopping	Power,	$dK/d(\rho_0 l)$	range, $\rho_0 l$	20 col3/col4
MeV	electronic(e)	MeV cm ² /gm nuclear(n)	total(t)	gm/cm ²	n-prob.
20	2.331E+01	1.006E-02	2.332E+01	4.756E-01	0.00862
40	1.331E+01	5.221E-03	1.331E+01	1.662E+00	0.00784
60	9.642E+00	3.553E-03	9.645E+00	3.453E+00	0.00736
80	7.714E+00	2.703E-03	7.717E+00	5.786E+00	0.00700
100	6.518E+00	2.186E-03	6.520E+00	8.616E+00	0.00670
120	5.701E+00	1.838E-03	5.703E+00	1.190E+01	0.00644
140	5.107E+00	1.587E-03	5.109E+00	1.561E+01	0.00621
160	4.655E+00	1.398E-03	4.656E+00	1.971E+01	0.00600
180	4.299E+00	1.250E-03	4.301E+00	2.418E+01	0.00581
200	4.013E+00	1.130E-03	4.014E+00	2.900E+01	0.00563
sum					0.06761

TABLE II. Stopping power for protons stopping in graphite, density 1.70 gm/cm², NIST[42]. Col6 gives the probability of nuclear scatter in the approximation that nuclear energy loss (in this energy range) is always negligible compared to electric energy loss. The binning error associated with quite wide kinetic energy bins is quite small because the probabilities vary slowly. Though the polarization detection efficiency E , is 7% percent, the analyzing power will exceed, say 70%, only for, perhaps, an order of magnitude smaller efficiency.

sum rule, arXiv:nucl-ex/0603021v3 29 Mar 2006, and Physikalisches Institut, Universitat Erlangen-N, 2018

- [22] J. Bystricky, F. Lehar, and P. Winternitz, *On tests of time reversal invariance in nucleon-nucleon scattering*, *Journale de Physique*, **45**, 2, pp 207-224, 1984
- [23] C. Wilkin, *The legacy of the experimental hadron physics program at COSY*, *Eur. Phys. J. A* **53** (2017 114, 2017
- [24] D. Eversmann et al., *New method for a continuous determination of the spin tune in storage rings and implications for precision experiments*, *Phys. Rev. Lett.* **115** 094801, 2015
- [25] N. Hempelmann et al., *Phase-locking the spin precession in a storage ring*, *P.R.L.* **119**, 119401, 2017
- [26] F. Rathmann, N. Nikoliev, and J. Slim, *Spin dynamics investigations for the electric dipole moment experiment*, *Phys. Rev. Accel. Beams* **23**, 024601, 2020
- [27] J. Slim et al., *First detection of collective oscillations of a stored deuteron beam with an amplitude close to the quantum limit*, *Phys. Rev. Accel. Beams*, **24**, 124601, 2021
- [28] F. Rathmann, *First direct hadron EDM measurement with deuterons using COSY*, Willy Haeberli Memorial Symposium, <https://www.physics.wisc.edu/haeberli-symposium>, 2022
- [29] R. Talman, *Improving the hadron EDM upper limit using doubly-magic proton and helion beams*, arXiv:2205.10526v1 [physics.acc-ph] 21 May, 2022
- [30] R. Talman and N. N. Nikolaev, *Colliding beam elastic p, p and p, d scattering to test T- and P-violation*, Snowmass 2021, Community Town Hall/86, 5 October, 2020
- [31] P. Lenisa et al., *Low-energy spin-physics experiments with polarized beams and targets at the COSY storage ring*, *EPJ Techniques and Instrumentation*, <https://doi.org/10.1140/epjti/s40485-019-0051-y>, 2019
- [32] M. Han and Y. Nambu, *Three-Triplet Model with Double SU(3) Symmetry*, *Phys. Rev.* **129**, 4B, 1965
- [33] A.D. Sakharov, *Violation of CP invariance, C asymmetry, and baryon asymmetry of the universe*, *JETP Lett.* **5**, 24-27, 1967
- [34] F. Arash, M. Moravcsik, and G. Goldstein, *Dynamics-independent Null, experiment for testing time-reversal independence*, *Phys. Rev. Lett.*, **54**, 2649, 1985
- [35] L. Stodolsky, *Nucl. Phys.*, *Parity violation in threshold neutron scattering*, **B197**, 213, 1982
- [36] M. Ieira, et al., *A multifoil carbon polarimeter for protons between 20 and 84 MeV*, *Nuclear Instruments and Methods in Physics Research*, **A257**, 253-278, 1987
- [37] G.R. Plottner and A.D. Bocher, *Absolute calibration of spin 1/2 polarization*, *Phys. Lett.* **36B**, 3, 211, 1971
- [38] B. von Przewoski, et al., *Absolute measurement of the p +p analyzing power at 183 MeV*, *Phys. Rev. C*, **44**, 1, p44, 1991
- [39] Z. Bagdasarian et al., *Measurement of the analyzing power in proton-proton elastic scattering at small angles*, *Physics Letters B*, **739**, 152, 2014
- [40] J.D. Jackson and J.M. Blatt, *The interpretation of low energy proton-proton scattering*, *Rev. Mod. Phys.* **22**, 1, 77, 1950
- [41] Feenberg and E. Wigner, *Symmetry properties of Nuclear levels*, *Repts. Progr. in Phys.*, **8**, 274, 1941
- [42] National Bureau of Standards Physical Measurement Laboratory, <https://physics.nist.gov>
- [43] Julius Stratton, *Electromagnetic Theory*, McGraw-Hill, Book Company, Inc., 1941